Quark-mass and $1/N_c$ corrections to the vector-meson pseudoscalar-meson photon ($VP\gamma$) interaction

H. C. Lange, A. Krasniqi, and S. Scherer

Institut für Kernphysik, Johannes Gutenberg-Universität Mainz, D-55099 Mainz, Germany

(Received 17 November 2021; accepted 10 February 2022; published 1 March 2022)

We analyze quark-mass and $1/N_c$ corrections to all of the radiative transitions between the vector-meson nonet and the pseudoscalar-meson nonet within a chiral effective Lagrangian approach. We perform fits of the available coupling constants to experimental data and discuss the corresponding approximations. In terms of five (six) coupling constants, we obtain a reasonably good description of the twelve experimental decay rates.

DOI: 10.1103/PhysRevD.105.054001

I. INTRODUCTION

Because of chiral symmetry and its spontaneous symmetry breaking in the ground state of quantum chromodynamics (QCD) [1], the members of the lowest-lying pseudoscalar octet (π, K, η_8) play a special role: they are the Goldstone bosons [2,3] of QCD and would be exactly massless for massless quarks. In the large-number-of-colors (large-N_c) expansion, one considers QCD with quarks having N_c colors transforming under the fundamental representation of an SU(N_c) gauge group with gauge coupling parameter g. In the large-N_c limit [4,5], i.e., $N_c \to \infty$ with $g^2 N_c$ fixed, also the singlet eta, η_1, would be a Goldstone boson and would combine with the octet into a nonet of massless Goldstone bosons [6,7]. In the real world with $N_c = 3$, the masses of the light pseudoscalars originate from an explicit symmetry breaking due to the quark masses [1] and from the anomaly [8,9] of the singlet axial-vector current [10–12]. Chiral perturbation theory (ChPT) [13–15] provides a systematic method of analyzing the low-energy interactions of the octet Goldstone bosons among each other and with external sources (see, e.g., Refs. [16–18] for an introduction). The dynamical variables of ChPT are the Goldstone bosons rather than the quarks and gluons of QCD. By considering the combined chiral and large-N_c limits, it is possible to set up large-N_c ChPT as the effective field theory of QCD at low energies including the singlet field [19–28].

Chiral symmetry also constrains the interactions of Goldstone bosons with heavier, i.e., non-Goldstone-boson hadrons, however, setting up a consistent power-counting scheme turns out to be more complex (see, e.g., Refs. [29–37]). Ever since the pioneering works on nonlinear realizations of chiral symmetry [38–40], there have been numerous approaches to the construction of chiral effective Lagrangians including vector mesons (see, e.g., Refs. [14,41–51]). They differ by, first, how the Lorentz group acts on the dynamical fields representing the vector mesons, either in terms of a vector field V^μ [52,53] or in terms of an antisymmetric second-rank tensor field $T^{\mu\nu}$ [54,55], and, second, how the chiral group operates on the SU(3) flavor degrees of freedom of the vector mesons. The vector-meson pseudoscalar-meson photon ($VP\gamma$) interaction responsible for, e.g., the radiative decay of a vector meson into a pseudoscalar meson is complementary to the hadronic decay of a vector meson into two pseudoscalar mesons, because it probes the so-called odd-intrinsic-parity sector of low-energy QCD. In the present case, this refers to the odd number of Goldstone bosons, namely, one, participating in the interaction with a single vector meson and a photon. Starting with the early predictions based on SU(3) symmetry [56], radiative decays of vector mesons into pseudoscalar mesons were studied in a large number of approaches (for a review of earlier work, see Ref. [57]). Naming just a few, these include investigations in the framework of the quark model [58,59], phenomenological Lagrangians [60,61], chiral effective Lagrangians [35,62–69], QCD sum rules [70–72], and lattice QCD [73–77].

In this work, we perform a comprehensive study of all radiative transitions between the vector-meson nonet and the pseudoscalar-meson nonet in the framework of a chiral effective Lagrangian in the vector formulation, including $1/N_c$ and quark-mass corrections of first order. We perform fits of the available coupling constants to experimental data and discuss the corresponding approximations. In terms of five (six) coupling constants, we obtain a reasonably good description of the 12 experimental decay rates. In Sec. II, we describe the chiral effective Lagrangian and the mixing

of singlet and octet fields. Section III contains our convention of the invariant amplitude and the calculation of the decay rate. In Sec. IV, we present the results of our fits for different levels of approximation. Finally, in Sec. V, we conclude with a few remarks.

II. EFFECTIVE LAGRANGIAN

In our approach, we assume that the decay rates are continuous functions of N_c^{-1} and m for $N_c^{-1} \geq 0$ and $m \geq 0$, where m collectively denotes the light-quark masses. This implies that the decay rates have a finite limit as $N_c \to \infty$ and $m \to 0$ and that this limit does not depend on the order of the LN_c and chiral limits.[1] Since we are working at the tree level, our results will not only automatically fulfill this condition, but can even be written as a power series in N_c^{-1} and m. Of course, when calculating chiral loop corrections, one will also pick up nonanalytical terms in the quark masses of the type $m\ln(m)$ [14,15] which, however, still vanish for m approaching zero.

In this section, we discuss the leading-order (LO) Lagrangian and its next-to-leading-order (NLO) $1/N_c$ and quark-mass corrections. The pseudoscalar dynamical degrees of freedom are collected in the unitary 3×3 matrix

$$U(x) = \exp\left(i\frac{\Phi(x)}{F}\right). \tag{1}$$

In Eq. (1), F denotes the pion-decay constant in the three-flavor chiral limit of vanishing quark masses, $m_u = m_d = m_s = 0$, and is counted as $F = \mathcal{O}(\sqrt{N_c})$ in the large-N_c limit [11].[2] In our numerical analysis we take $F = 90.9$ MeV (see Eq. (36) and Table II below). The Hermitian 3×3 matrix

$$\Phi = \sum_{a=1}^{8} \lambda_a \phi_a + \lambda_0 \phi_0 = \hat{\Phi} + \tilde{\Phi} = \begin{pmatrix} \pi^0 + \frac{1}{\sqrt{3}}\eta_8 + \sqrt{\frac{2}{3}}\eta_1 & \sqrt{2}\pi^+ & \sqrt{2}K^+ \\ \sqrt{2}\pi^- & -\pi^0 + \frac{1}{\sqrt{3}}\eta_8 + \sqrt{\frac{2}{3}}\eta_1 & \sqrt{2}K^0 \\ \sqrt{2}K^- & \sqrt{2}\bar{K}^0 & -\frac{2}{\sqrt{3}}\eta_8 + \sqrt{\frac{2}{3}}\eta_1 \end{pmatrix} \tag{2}$$

contains the pseudoscalar octet fields π, K, η_8 and the pseudoscalar singlet field η_1, the λ_a ($a = 1, \ldots, 8$) are the Gell-Mann matrices, and $\lambda_0 \equiv \sqrt{2/3}\mathbb{1}$. The pseudoscalar fields $\phi_0(x), \ldots, \phi_8(x)$ count as $\mathcal{O}(\sqrt{N_c})$ such that in combination with $F = \mathcal{O}(\sqrt{N_c})$ the matrix U is of $\mathcal{O}(N_c^0)$.

In this work, we describe the vector-meson degrees of freedom within the so-called vector-field formalism [47,51,52]. To that end we collect the vector fields in a Hermitian 3×3 matrix similar to Eq. (1),[3]

$$V_\mu = \left(\sum_{a=1}^{8} \frac{\lambda_a}{2} V_a + \frac{\lambda_0}{2} V_0\right)_\mu = \hat{V}_\mu + \tilde{V}_\mu = \frac{1}{2}\begin{pmatrix} \rho^0 + \frac{1}{\sqrt{3}}\omega_8 + \sqrt{\frac{2}{3}}\omega_1 & \sqrt{2}\rho^+ & \sqrt{2}K^{*+} \\ \sqrt{2}\rho^- & -\rho^0 + \frac{1}{\sqrt{3}}\omega_8 + \sqrt{\frac{2}{3}}\omega_1 & \sqrt{2}K^{*0} \\ \sqrt{2}K^{*-} & \sqrt{2}\bar{K}^{*0} & -\frac{2}{\sqrt{3}}\omega_8 + \sqrt{\frac{2}{3}}\omega_1 \end{pmatrix}_\mu . \tag{3}$$

In order to construct a chirally invariant Lagrangian, we follow Gasser and Leutwyler by promoting the global $\mathrm{U}(3)_L \times \mathrm{U}(3)_R$ symmetry of QCD to a local one [15] (see, e.g., Ref [18] for a discussion). In this process, we introduce external fields s, p, l_μ, and r_μ which are Hermitian, color-neutral 3×3 matrices coupling to the corresponding quark bilinears. In addition, we introduce a real field θ coupling to the winding number density. Introducing $u = \sqrt{U}$, the chiral vielbein u_μ and the field-strength tensors $f_{\pm\mu\nu}$ are defined by [18,46,47]

$$\begin{aligned} u_\mu &= i[u^\dagger(\partial_\mu - ir_\mu)u - u(\partial_\mu - il_\mu)u^\dagger], \\ f_{\pm\mu\nu} &= u f_{L\mu\nu} u^\dagger \pm u^\dagger f_{R\mu\nu} u, \end{aligned} \tag{4}$$

where l_μ and r_μ denote external fields which couple to the corresponding currents in three-flavor QCD [15]. In the present work, these external fields, eventually, will contain

[1] Setting up an effective theory for baryons is more complex, because there is more than one phenomenologically viable way to take a large-N_c limit [78] and, moreover, the result of a combined large-N_c and chiral limit may depend on the path how this limit is taken [79].

[2] Here, we deviate from the often-used convention of indicating the *three*-flavor chiral limit by a subscript 0.

[3] Note that we include an additional factor $1/2$.

the electromagnetic four-vector potential, and $f_{L\mu\nu}$ and $f_{R\mu\nu}$ are the corresponding field-strength tensors,

$$f_{L\mu\nu} = \partial_\mu l_\nu - \partial_\nu l_\mu - i[l_\mu, l_\nu],$$
$$f_{R\mu\nu} = \partial_\mu r_\nu - \partial_\nu r_\mu - i[r_\mu, r_\nu].$$

A. Lagrangian of the pseudoscalar mesons

We first specify the Lagrangian of the pseudoscalar sector which is relevant at next-to-leading order (see Ref. [28] for more details). The effective Lagrangian is organized as a *simultaneous* expansion in terms of momenta p, quark masses m, and $1/N_c$. Here, we follow Ref. [20] and count the three expansion variables as small quantities of order

$$p = \mathcal{O}(\sqrt{\delta}), \qquad m = \mathcal{O}(\delta), \qquad 1/N_c = \mathcal{O}(\delta), \quad (5)$$

where δ denotes a common expansion parameter. It is understood that dimensionful quantities such as p and m need to be small in comparison with an energy scale. We only specify the terms appearing in the calculation of the masses, the wave function renormalization constants, the decay constants, and the mixing [28]. The leading-order Lagrangian is given by [20,22]

$$\mathcal{L}^{(0)} = \frac{F^2}{4}\langle D_\mu U D^\mu U^\dagger\rangle + \frac{F^2}{4}\langle \chi U^\dagger + U\chi^\dagger\rangle - \frac{1}{2}\tau\left(\sqrt{6}\frac{\eta_1}{F} + \theta\right)^2, \quad (6)$$

where the symbol $\langle\rangle$ denotes the trace over flavor indices. The covariant derivatives are defined as

$$D_\mu U = \partial_\mu U - i r_\mu U + i U l_\mu,$$
$$D_\mu U^\dagger = \partial_\mu U^\dagger + i U^\dagger r_\mu - i l_\mu U^\dagger. \quad (7)$$

In Eq. (6), $\chi = 2B_0(s + ip)$ contains the external scalar and pseudoscalar fields [15]. The low-energy constant (LEC) B_0 is related to the scalar singlet quark condensate $\langle\bar{q}q\rangle_0$ in the three-flavor chiral limit and is of $\mathcal{O}(N_c^0)$ [20]. For the purposes of this work we replace $\chi \to 2B_0\mathcal{M}$, where $\mathcal{M} = \mathrm{diag}(m_u, m_d, m_s)$ is the quark-mass matrix. Moreover, we neglect effects from isospin symmetry breaking, i.e., we work in the isospin symmetric limit $m_u = m_d = \hat{m}$. The constant $\tau = \mathcal{O}(N_c^0)$ is the topological susceptibility of the purely gluonic theory [20]. We set the vacuum angle $\theta(x)$ to zero, corresponding to the absence of P and CP violation in QCD [15].

For an introduction to the large-N_c counting, we refer, e.g., to Refs. [28,80,81]. According to Ref. [81], the leading contribution to a correlation function of quark bilinears is of order N_c and contains a single quark loop. The summation over the quark flavors running in the loop amounts to taking a single flavor trace over the product of (flavor) λ matrices that belong to the quark bilinears. Therefore, the leading-order terms of the effective Lagrangian are also expected to be single-trace terms. Similarly, diagrams with two quark loops have two flavor traces and are down by one order of $1/N_c$. Accordingly, double-trace terms in the effective Lagrangian are expected to be suppressed by one order of $1/N_c$. A subtlety arises because of the so-called trace relations [82] relating linear combinations of single-trace and multiple-trace terms such that the naive counting may require a more thorough analysis (see Ref. [14], Sec. 13). Taking $F = \mathcal{O}(\sqrt{N_c})$ into account, the first term of $\mathcal{L}^{(0)}$ is of $\mathcal{O}(p^2 m^0 N_c)$, the second of $\mathcal{O}(p^0 m N_c)$, and the third of $\mathcal{O}(p^0 m^0 N_c^0)$, i.e., all terms are of $\mathcal{O}(\delta^0)$.

The relevant terms of the next-to-leading-order Lagrangian are given by [22]

$$\mathcal{L}^{(1)} = L_5\langle D_\mu U D^\mu U^\dagger(\chi U^\dagger + U\chi^\dagger)\rangle + L_8\langle \chi U^\dagger \chi U^\dagger + U\chi^\dagger U\chi^\dagger\rangle + \frac{1}{2}\Lambda_1 D_\mu\eta_1 D^\mu\eta_1 - i\frac{F^2}{12}\Lambda_2\left(\sqrt{6}\frac{\eta_1}{F} + \theta\right)\langle \chi U^\dagger - U\chi^\dagger\rangle + \ldots, \quad (8)$$

where

$$D_\mu\eta_1 = \partial_\mu\eta_1 - \sqrt{\frac{2}{3}}F\langle a_\mu\rangle, \quad (9)$$

$$a_\mu = \frac{1}{2}(r_\mu - l_\mu), \quad (10)$$

and the ellipsis refers to the suppressed terms. The LECs L_5 and L_8 are of $\mathcal{O}(N_c)$ [15] such that the first and second term of $\mathcal{L}^{(1)}$ count as $\mathcal{O}(p^2 m N_c)$ and $\mathcal{O}(p^0 m^2 N_c)$, respectively. The LECs Λ_1 and Λ_2 represent quantities of $\mathcal{O}(N_c^{-1})$ [22] such that the third term is of $\mathcal{O}(p^2 m^0 N_c^0)$ and the fourth of $\mathcal{O}(p^0 m N_c^0)$. Therefore, all expressions of $\mathcal{L}^{(1)}$ are of order $\mathcal{O}(\delta)$.

B. Lagrangian of the vector mesons

In the present case we are not interested in the interaction of vector mesons among each other. Introducing the chiral covariant derivative of the vector-meson fields as

$$D_\mu V_\nu = \partial_\mu V_\nu + [\Gamma_\mu, V_\nu], \quad (11)$$

where the chiral connection is given by [18]

$$\Gamma_\mu = \frac{1}{2}[u^\dagger(\partial_\mu - i r_\mu)u + u(\partial_\mu - i l_\mu)u^\dagger], \quad (12)$$

we define the field-strength tensor as

$$V_{\mu\nu} = D_\mu V_\nu - D_\nu V_\mu. \tag{13}$$

The leading-order Lagrangian is then given by

$$\mathcal{L}_V = -\frac{1}{2}\langle V_{\mu\nu} V^{\mu\nu}\rangle + m_V^2 \langle V_\mu V^\mu\rangle, \tag{14}$$

where m_V denotes the leading-order mass common to all vector-meson fields. We now include NLO corrections to the mass terms of $\mathcal{O}(N_c^{-1})$ and $\mathcal{O}(m)$, respectively,[4]

$$\mathcal{L} = \frac{1}{3}\Delta m_S^2 \langle V_\mu\rangle\langle V^\mu\rangle + \frac{c_\chi}{2}\langle \chi_+ V_\mu V^\mu\rangle, \tag{15}$$

where χ_+ is defined as

$$\chi_+ = u^\dagger \chi u^\dagger + u\chi^\dagger u. \tag{16}$$

C. Leading-order interaction Lagrangian

In terms of the building blocks above, the leading-order Lagrangian, giving rise to the $VP\gamma$ interaction, is given by

$$\mathcal{L}_{\mathrm{LO}} = c_1 \epsilon^{\mu\nu\rho\sigma}\langle f_{+\mu\nu}\{V_\rho, u_\sigma\}\rangle, \tag{17}$$

where $\epsilon_{0123} = 1$ and c_1 is a dimensionless coupling constant. Since $\epsilon^{\mu\nu\rho\sigma}$ and u_σ are Lorentz pseudotensors of rank 4 and 1, respectively, and $f_{+\mu\nu}$ and V_ρ are Lorentz tensors of rank 2 and 1, respectively, the Lagrangian of Eq. (17) is even under parity. Moreover, the anticommutator is required in Eq. (17) to generate positive charge-conjugation parity (see, e.g., Ref. [18] for more details).

In order to describe the coupling to an external electromagnetic field, we insert $l_\mu = r_\mu = -eQA_\mu$, where $e > 0$ is the proton charge ($e^2/(4\pi) \approx 1/137$), Q denotes the quark-charge matrix, and A_μ is the electromagnetic four-vector potential. Regarding the large-N_c behavior of Q, we make use of the form proposed by Bär and Wiese [83]. They pointed out that, when considering the electromagnetic interaction of quarks with an arbitrary number of colors, the cancelation of triangle anomalies in the large-N_c Standard Model requires the following replacement of the ordinary quark-charge matrix,

$$Q = \begin{pmatrix} \frac{2}{3} & 0 & 0 \\ 0 & -\frac{1}{3} & 0 \\ 0 & 0 & -\frac{1}{3} \end{pmatrix} \to \begin{pmatrix} \frac{1}{2N_c} + \frac{1}{2} & 0 & 0 \\ 0 & \frac{1}{2N_c} - \frac{1}{2} & 0 \\ 0 & 0 & \frac{1}{2N_c} - \frac{1}{2} \end{pmatrix}$$
$$= \begin{pmatrix} \frac{1}{2} & 0 & 0 \\ 0 & -\frac{1}{2} & 0 \\ 0 & 0 & -\frac{1}{2} \end{pmatrix} + \frac{1}{2N_c}\mathbb{1} \equiv Q_0 + Q_1. \tag{18}$$

Expanding the building blocks in the Goldstone-boson fields and keeping only the linear term in the expansion amounts to the replacements

$$f_{+\mu\nu} \to -2eQF_{\mu\nu}, \qquad u_\sigma \to -\frac{\partial_\sigma \Phi}{F}, \tag{19}$$

where $F_{\mu\nu} = \partial_\mu A_\nu - \partial_\nu A_\mu$ is the electromagnetic field-strength tensor. Thus, the LO $VP\gamma$ interaction Lagrangian, obtained from a nonlinearly realized chiral symmetry, reads

$$\mathcal{L}_{\mathrm{LO}}^{VP\gamma} = 2e\frac{c_1}{F}\epsilon^{\mu\nu\rho\sigma} F_{\mu\nu}\langle Q\{V_\rho, \partial_\sigma\Phi\}\rangle. \tag{20}$$

The expansion of Eq. (20) in terms of the singlet and octet fields is given in the Appendix. When inserting Eq. (18) for the quark-charge matrix into Eq. (20), we obtain the leading-order contribution proportional to Q_0 and a $1/N_c$ correction proportional to Q_1. When discussing our results in Sec. IV, we will keep both scenarios in mind, i.e., we will compare the results obtained from using the physical quark-charge matrix Q with $N_c = 3$ with the expanded version truncated at order $1/N_c$ and putting $N_c = 3$ at the end.

D. Next-to-leading-order interaction Lagrangian

The NLO $1/N_c$ corrections to the Lagrangian of Eq. (17) are obtained in terms of expressions involving two flavor traces of the same building blocks,

$$\mathcal{L}_{\mathrm{NLO},1/N_c} = c_2\epsilon^{\mu\nu\rho\sigma}\langle V_\rho\rangle\langle f_{+\mu\nu}u_\sigma\rangle + c_3\epsilon^{\mu\nu\rho\sigma}\langle f_{+\mu\nu}V_\rho\rangle\langle u_\sigma\rangle + c_4\epsilon^{\mu\nu\rho\sigma}\langle f_{+\mu\nu}\rangle\langle V_\rho u_\sigma\rangle. \tag{21}$$

Performing the replacements of Eq. (19), we obtain from Eq. (21) the $1/N_c$ correction to the $VP\gamma$ interaction Lagrangian,

$$\mathcal{L}_{\mathrm{NLO},1/N_c}^{VP\gamma} = 2\frac{e}{F}\epsilon^{\mu\nu\rho\sigma}F_{\mu\nu}(c_2\langle V_\rho\rangle\langle Q\partial_\sigma\Phi\rangle + c_3\langle QV_\rho\rangle\langle\partial_\sigma\Phi\rangle + c_4\langle Q\rangle\langle V_\rho\partial_\sigma\Phi\rangle). \tag{22}$$

The first (c_2) term contributes to the singlet vector meson transitions, the second (c_3) term to the singlet pseudoscalar transitions, and the last (c_4) term vanishes for physical

[4]For the sake of simplicity, we do not include corrections of the kinetic term. Δm_S^2 and c_χ are of order $\mathcal{O}(N_c^{-1})$ and $\mathcal{O}(N_c^0)$, respectively.

quark charges, because $\langle Q\rangle = 0$ in this case. For the expressions in terms of the singlet and octet fields, see Appendix. For $N_c = 3$, the Lagrangians of Eqs. (20) and (22) do not generate a singlet-to-singlet transition. This is a result of SU(3) symmetry [60], because the electromagnetic current operator, consisting of octet components, cannot couple a singlet to a singlet. This argument no longer works for general N_c, because the electromagnetic current operator now also develops a singlet component.

Finally, we consider quark-mass corrections in terms of the building blocks

$$\chi_\pm = u^\dagger \chi u^\dagger \pm u \chi^\dagger u. \tag{23}$$

Considering only single-trace terms, the quark-mass corrections are given by

$$\begin{aligned}\mathcal{L}_{\mathrm{NLO},\chi} = {} & c_5 \epsilon^{\mu\nu\rho\sigma} \langle \chi_+ f_{+\mu\nu} \{V_\rho, u_\sigma\}\rangle \\ & + c_6 \epsilon^{\mu\nu\rho\sigma} \langle \chi_+ V_\rho f_{+\mu\nu} u_\sigma + \chi_+ u_\sigma f_{+\mu\nu} V_\rho\rangle \\ & + i c_7 \epsilon^{\mu\nu\rho\sigma} \langle \{f_{+\mu\nu}, \partial_\rho V_\sigma\} \chi_-\rangle \\ & + i c_8 \epsilon^{\mu\nu\rho\sigma} \langle f_{-\mu\nu} [\partial_\rho V_\sigma, \chi_+]\rangle. \end{aligned} \tag{24}$$

Again, making the replacements of Eq. (19), in combination with

$$\chi_+ \to 4B_0 \mathcal{M}, \quad \chi_- \to -2i \frac{B_0}{F} \{\mathcal{M}, \Phi\}, \quad f_{-\mu\nu} \to i \frac{e}{F} F_{\mu\nu} [Q, \Phi], \tag{25}$$

and performing a partial integration, we obtain from Eq. (24) the first-order quark-mass correction to the $VP\gamma$ interaction Lagrangian,

$$\begin{aligned}\mathcal{L}^{VP\gamma}_{\mathrm{NLO},\chi} = {} & 4B_0 \frac{e}{F} \epsilon^{\mu\nu\rho\sigma} F_{\mu\nu} (c_+ \langle \{Q, V_\rho\} \{\mathcal{M}, \partial_\sigma \Phi\}\rangle \\ & + c_- \langle [Q, \partial_\sigma \Phi][V_\rho, \mathcal{M}]\rangle), \end{aligned} \tag{26}$$

where $c_+ = c_5 + c_6 - c_7$ and $c_- = c_5 - c_6 - c_8$. As we will see later on, the c_- term contributes only to the radiative transition of the $K^{*\pm}$.

At this stage, we have collected the relevant Lagrangians including the leading $1/N_c$ and quark-mass corrections. Note that we consider corrections of the type $1/N_c \times \chi$ as of higher order.

E. Field renormalization and mixing

Before turning to the evaluation of the transition matrix element, we need to address two issues. First, the Lagrangians of the previous sections were expressed in terms of bare fields. Although we are only working at the tree level, the terms proportional to L_5 and Λ_1 contribute to the field renormalization constants. Second, the breaking of SU(3) symmetry due to the quark masses as well as the chiral anomaly generate a mixing of the singlet and octet fields. We neglect effects from isospin symmetry breaking, i.e., we work in the isospin symmetric limit $m_u = m_d = \hat{m}$.

To the order we are considering, the connection between the bare pion/kaon fields ϕ_i and the renormalized pion/kaon fields ϕ_i^R is given by

$$\begin{aligned}\phi_i &= \sqrt{Z_\pi}\phi_i^R, \quad \sqrt{Z_\pi} = 1 - 4\frac{\mathring{M}_\pi^2}{F^2} L_5, \quad i = 1,2,3, \\ \phi_i &= \sqrt{Z_K}\phi_i^R, \quad \sqrt{Z_K} = 1 - 4\frac{\mathring{M}_K^2}{F^2} L_5, \quad i = 4,5,6,7, \end{aligned} \tag{27}$$

where $\mathring{M}_\pi^2 = 2B_0\hat{m}$ and $\mathring{M}_K^2 = (m_s + \hat{m})B_0$ denote the lowest-order predictions for the squared pion and kaon masses, respectively. For the expression of the mixing of the pseudoscalar fields, we make use of the results of Ref. [28]. Denoting the bare fields by η_1 and η_8 and the renormalized physical fields by η^R and η'^R, we make use of

$$\begin{aligned}\eta_8 = {} & \left[\left(1 - \frac{1}{2}\delta_8\right)\cos(\theta_P) + \frac{1}{2}\delta_{81}\sin(\theta_P)\right]\eta^R \\ & + \left[\left(1 - \frac{1}{2}\delta_8\right)\sin(\theta_P) - \frac{1}{2}\delta_{81}\cos(\theta_P)\right]\eta'^R, \\ \eta_1 = {} & \left[-\frac{1}{2}\delta_{81}\cos(\theta_P) - \left(1 - \frac{1}{2}\delta_1\sin(\theta_P)\right)\right]\eta^R \\ & + \left[-\frac{1}{2}\delta_{81}\sin(\theta_P) + \left(1 - \frac{1}{2}\delta_1\right)\cos(\theta_P)\right]\eta'^R, \end{aligned} \tag{28}$$

where

$$\begin{aligned}\delta_8 &= \frac{8(4\mathring{M}_K^2 - \mathring{M}_\pi^2)}{3F^2} L_5, \\ \delta_1 &= \frac{8(2\mathring{M}_K^2 + \mathring{M}_\pi^2)}{3F^2} L_5 + \Lambda_1, \\ \delta_{81} &= -\frac{16\sqrt{2}(\mathring{M}_K^2 - \mathring{M}_\pi^2)}{3F^2} L_5. \end{aligned}$$

Using the numerical values for the masses and low-energy constants from the next subsection, we obtain for the pseudoscalar mixing angle the values $\theta_P^{[0]} = -19.7°$ and $\theta_P^{[1]} = -12.4°$ at leading order and next-to-leading order, respectively. These values are representative and cover the range for θ_P between $-10°$ and $-20°$ reported in Ref. [84].

In the case of the vector mesons, we only consider $\phi - \omega$ mixing in the form

$$\begin{pmatrix}\phi \\ \omega\end{pmatrix} = \begin{pmatrix}\cos(\theta_V) & -\sin(\theta_V) \\ \sin(\theta_V) & \cos(\theta_V)\end{pmatrix}\begin{pmatrix}\omega_8 \\ \omega_1\end{pmatrix} \equiv R_V \begin{pmatrix}\omega_8 \\ \omega_1\end{pmatrix}. \tag{29}$$

The diagonal mass matrix of the physical fields is related to the symmetric mass matrix in the octet-singlet basis, including the NLO corrections of $\mathcal{O}(N_c^{-1})$ and $\mathcal{O}(m)$, via

$$\mathcal{M}^2_{V,\text{phys}} = \begin{pmatrix} m_\phi^2 & 0 \\ 0 & m_\omega^2 \end{pmatrix} = R_V \begin{pmatrix} m_8^2 & m_{81}^2 \\ m_{81}^2 & m_1^2 \end{pmatrix} R_V^T, \tag{30}$$

where, to the order we are working at,

$$\begin{aligned} m_8^2 &= m_V^2 + \frac{c_\chi}{3}(4\mathring{M}_K^2 - \mathring{M}_\pi^2), \\ m_1^2 &= m_V^2 + \Delta m_S^2 + \frac{c_\chi}{3}(\mathring{M}_\pi^2 + 2\mathring{M}_K^2), \\ m_{18}^2 &= -\frac{2\sqrt{2}c_\chi}{3}(\mathring{M}_K^2 - \mathring{M}_\pi^2). \end{aligned}$$

The mixing angle is obtained from the relation

$$\tan(\theta_V) = \sqrt{\frac{m_\phi^2 - m_8^2}{m_8^2 - m_\omega^2}}, \tag{31}$$

where m_8^2 satisfies, to the order we are working at,

$$m_8^2 = \frac{1}{3}(4m_{K^*}^2 - m_\rho^2),$$

resulting in

$$\tan(\theta_V) = \sqrt{\frac{3m_\phi^2 + m_\rho^2 - 4m_{K^*}^2}{4m_{K^*}^2 - m_\rho^2 - 3m_\omega^2}}.$$

For the mixing angle we obtain $\theta_V = 39.8°$, which turns out to be close to the ideal mixing $\theta_V = 35.3°$, corresponding to $\phi = -s\bar{s}$ and $\omega = (u\bar{u} + d\bar{d})/\sqrt{2}$ in the quark model,

$$\begin{aligned} \phi_{\text{ideal}} &= \sqrt{\frac{2}{3}}\omega_8 - \frac{1}{\sqrt{3}}\omega_1, \\ \omega_{\text{ideal}} &= \frac{1}{\sqrt{3}}\omega_8 + \sqrt{\frac{2}{3}}\omega_1. \end{aligned} \tag{32}$$

F. Numerical values for masses and parameters

For the empirical masses of the pseudoscalar mesons and the vector mesons we make use of the values given in Table I [84]. For the decay constants we take $F_\pi = 92.2$ MeV and $F_K = 110.$ MeV [84].[5] The predictions for the squared pion and kaon masses are obtained from the one-loop expressions of chiral perturbation theory [15,17] by dropping the loop contributions and the tree-level contributions proportional to L_6 and L_4,

TABLE I. Masses of the pseudoscalar mesons and the vector mesons in MeV.

$M_{\pi^\pm}$	M_{π^0}	$M_{K^\pm}$	$M_{K^0/\bar{K}^0}$	M_η	$M_{\eta'}$
139.6	135.0	493.7	497.6	547.9	957.8
$m_{\rho^\pm}$	m_{ρ^0}	$m_{K^{*\pm}}$	$m_{K^{*0}/\bar{K}^{*0}}$	m_ω	m_ϕ
775.1	775.3	891.8	895.6	782.7	1019.5

$$\begin{aligned} M_\pi^2 &= 2B\hat{m}\left[1 + \frac{16B\hat{m}}{F^2}(2L_8 - L_5)\right], \\ M_K^2 &= B(m_s + \hat{m})\left[1 + \frac{8B(m_s + \hat{m})}{F^2}(2L_8 - L_5)\right]. \end{aligned}$$

In terms of the quark mass ratio r [84],

$$r = \frac{m_s}{\hat{m}} = 27.37, \tag{33}$$

we obtain for the lowest-order squared pion and kaon masses

$$\begin{aligned} \mathring{M}_\pi^2 &= \frac{r+1}{r-1}\bar{M}_\pi^2 + 4\frac{\bar{M}_K^2}{1-r^2}, \\ \mathring{M}_K^2 &= \frac{(1+r)^2\bar{M}_\pi^2 - 4\bar{M}_K^2}{2(r-1)}, \end{aligned} \tag{34}$$

where

$$\bar{M}_\pi = \frac{M_{\pi^0} + M_{\pi^\pm}}{2} \quad \text{and} \quad \bar{M}_K = \frac{M_{K^0} + M_{K^\pm}}{2}.$$

Using, in addition, the expressions for the pion and kaon decay constants F_π and F_K,

$$\begin{aligned} F_\pi &= F\left(1 + 4\frac{\mathring{M}_\pi^2}{F^2}L_5\right), \\ F_K &= F\left(1 + 4\frac{\mathring{M}_K^2}{F^2}L_5\right), \end{aligned} \tag{35}$$

we can write

$$\begin{aligned} F &= \frac{\mathring{M}_K^2 F_\pi - \mathring{M}_\pi^2 F_K}{\mathring{M}_K^2 - \mathring{M}_\pi^2}, \\ L_5 &= \frac{F(F_\pi - F)}{4\mathring{M}_\pi^2}, \\ L_8 &= \frac{F^2}{4(1-r^2)\mathring{M}_\pi^4}\left(\frac{1+r}{2}\bar{M}_\pi^2 - \bar{M}_K^2\right) + \frac{L_5}{2}. \end{aligned} \tag{36}$$

[5]Here and in the following, an integer followed by a point denotes a rounded number rather than an exact integer.

TABLE II. Numerical values of lowest-order pion and kaon masses and LECs.

$\mathring{M}_\pi$	$\mathring{M}_K$	F	L_5	L_8
137.7 MeV	518.7 MeV	90.9 MeV	1.62×10^{-3}	0.642×10^{-3}

The corresponding values for $\mathring{M}_\pi$, $\mathring{M}_K$, F, L_5, and L_8 are given in Table II.

III. INVARIANT MATRIX ELEMENT AND DECAY RATE

The invariant amplitude of the decay $V(p,\epsilon_V)\to P(k)+\gamma(q,\epsilon)$ may be parametrized as[6]

$$\mathcal{M}=-2ie\mathcal{A}\epsilon^{\mu\nu\rho\sigma}q_\mu\epsilon_\nu^*(q)\epsilon_{V\rho}(p)k_\sigma, \tag{37}$$

where four-momentum conservation $p=k+q$ is implied, ϵ and ϵ_V denote the polarization vectors of the photon and the vector meson, respectively, and the amplitude $\mathcal{A}$ is determined from the Lagrangians of Eqs. (20), (22), and (26). The invariant amplitude for the decay $P(k)\to V(p,\epsilon_V)+\gamma(q,\epsilon)$ is obtained from Eq. (37) by substituting $\epsilon_V\to\epsilon_V^*$ and $k\to -k$.

In the rest frame of the initial-state particle, the differential decay rate for the decay $A(p_A)\to B(p_B)+\gamma(q)$ is given by [85]

$$d\Gamma=\frac{1}{2m_A}\overline{|\mathcal{M}|^2}\frac{d^3p_B}{2E_B(2\pi)^3}\frac{d^3q}{2E_\gamma(2\pi)^3}(2\pi)^4\delta^4(p_A-p_B-q), \tag{38}$$

where E_B and E_γ denote the energies of the decay product B and the real photon, respectively. When averaging over the initial polarizations and summing over the final polarizations, we make use of the "completeness relations" [53] for the polarization vectors of the photon and the vector meson, respectively,[7]

$$\sum_{\lambda=\pm1}\epsilon_\nu^*(q,\lambda)\epsilon_{\nu'}(q,\lambda)=-g_{\nu\nu'},$$
$$\sum_{\lambda=-1}^{+1}\epsilon_{V\rho}(p,\lambda)\epsilon_{V\rho'}^*(p,\lambda)=\left(-g_{\rho\rho'}+\frac{p_\rho p_{\rho'}}{m_V^2}\right),$$

where m_V is the mass of the vector meson. Using [86]

$$\epsilon^{\mu\nu\rho\sigma}\epsilon^{\mu'}{}_{\nu'\rho'\sigma'}=-\det(g^{\alpha\alpha'}),\qquad \alpha=\mu,\rho,\sigma,\qquad \alpha'=\mu',\rho',\sigma',$$

in combination with the on-shell conditions $p_A^2=m_A^2$, $p_B^2=m_B^2$, and $q^2=0$, we obtain

$$\overline{|\mathcal{M}|^2}=c_A 2e^2|\mathcal{A}|^2(m_A^2-m_B^2)^2,$$

where $c_A=1/3$ for a vector meson in the initial state and $c_A=1$ for a pseudoscalar meson in the initial state. Using [53]

$$\frac{d^3q}{2E_\gamma}=d^4q\delta(q^2)\Theta(q_0),$$

we obtain for the decay rate

$$\begin{aligned}\Gamma_{A\to B\gamma}&=\frac{1}{2m_A}\int\frac{d^3p_B}{2E_B(2\pi)^3}\frac{d^3q}{2E_\gamma(2\pi)^3}(2\pi)^4\\&\quad\times\delta^4(p_A-p_B-q)\overline{|\mathcal{M}|^2}\\&=\frac{1}{16\pi^2m_A}\int\frac{d^3p_B}{E_B}\int d^4q\delta(q^2)\Theta(q_0)\\&\quad\times\delta^4(p_A-p_B-q)\overline{|\mathcal{M}|^2}\\&=c_A\frac{e^2|\mathcal{A}|^2}{8\pi}\left(\frac{m_A^2-m_B^2}{m_A}\right)^3.\end{aligned} \tag{39}$$

IV. RESULTS AND DISCUSSION

Starting from the expression for the decay rate, Eq. (39), we determine the low-energy coupling constants of the interaction Lagrangians by fitting the corresponding expressions to the available experimental data. For the masses of the pseudoscalar mesons and the vector mesons we make use of the values given in Table I. The experimental partial widths were calculated with the aid of the PDG values of the total widths in combination with the corresponding branching ratios [84] (see second column of Table III).

A. Leading order

In the following, we investigate different levels of approximation and compare the different scenarios. To that end, we start with the results corresponding to the leading-order Lagrangian of Eq. (20) in combination with the pseudoscalar mixing angle obtained at leading order, $\theta_P^{[0]}=-19.7°$, and the vector mixing angle corresponding to ideal mixing, i.e., $\cos(\theta_V)=\sqrt{2/3}$ and $\sin(\theta_V)=1/\sqrt{3}$. When fitting the data, we made use of the *Mathematica* package `NonLinearModelFit` [87]. In order to facilitate identifying which decays are well described and which are not, we introduce both a relative deviation and a deviation normalized with respect to the uncertainties as

[6]We follow the convention of Ref. [85] such that the invariant amplitude is obtained from $i\mathcal{L}_{\rm int}$.

[7]As usual it is assumed that the photon polarization vector is contracted with the matrix element of the conserved electromagnetic current.

TABLE III. Comparison of the decay rates at LO with experimental values [84].

Decay	Γ_{exp} (keV)	Γ_{LO} (keV)	Deviation δ_1	Deviation δ_2
$\rho^0 \to \pi^0\gamma$	$70. \pm 12.$	40.7 ± 5.4	-0.42	-2.3
$\rho^\pm \to \pi^\pm\gamma$	67.1 ± 7.5	40.4 ± 5.3	-0.40	-2.9
$\rho^0 \to \eta\gamma$	44.7 ± 3.1	33.7 ± 4.5	-0.25	-2.0
$\omega \to \pi^0\gamma$	$723. \pm 25.$	$364. \pm 48.$	-0.50	-6.6
$\omega \to \eta\gamma$	3.91 ± 0.35	4.07 ± 0.54	0.041	0.25
$\phi \to \pi^0\gamma$	5.61 ± 0.26	…	…	…
$\phi \to \eta\gamma$	55.4 ± 1.1	48.1 ± 6.4	-0.13	-1.1
$\phi \to \eta'\gamma$	0.2643 ± 0.0090	0.439 ± 0.058	0.66	3.0
$K^{*0} \to K^0\gamma$	$116. \pm 10.$	$91. \pm 12.$	-0.22	-1.6
$K^{*\pm} \to K^\pm\gamma$	50.4 ± 4.7	22.6 ± 3.0	-0.55	-5.0
$\eta' \to \rho^0\gamma$	55.5 ± 1.9	30.7 ± 4.1	-0.45	-5.6
$\eta' \to \omega\gamma$	4.74 ± 0.20	3.06 ± 0.40	-0.35	-3.7

$$\delta_1 = \frac{\Gamma_{\text{mod}} - \Gamma_{\text{exp}}}{\Gamma_{\text{exp}}}, \qquad \delta_2 = \frac{\Gamma_{\text{mod}} - \Gamma_{\text{exp}}}{\sqrt{\sigma_{\text{mod}}^2 + \sigma_{\text{exp}}^2}}. \quad (40)$$

Here, σ_{exp} and σ_{mod} denote the experimental uncertainty and the estimated model uncertainty, respectively. As a rule of thumb, values for $|\delta_2|$ larger than one indicate tension between the model and the experimental results. The result of the fit to the data is shown in Table III with $|c_1| = (3.82 \pm 0.25) \times 10^{-2}$. Note that because of the Okubo-Zweig-Iizuka (OZI) rule [88–90], at leading order, the decay rate for $\phi \to \pi^0\gamma$ vanishes as $N_c \to \infty$, independently from the value of the coupling constant c_1. Therefore, we have excluded this decay from the fit. Neglecting $\eta - \eta'$ mixing, i.e., taking $\theta_P = 0°$, the leading-order Lagrangian results generate the same ratios of the magnitudes of the decay amplitudes as the quark model with SU(6) symmetry [58].

In general, the numbers of the tables were rounded at the end of the calculation. Since the decay rate is a function of $|\mathcal{A}|^2$, it is not possible to extract the sign of c_1. For the sake of simplicity, we assume $c_1 > 0$ such that the signs of the remaining coupling constants, to be determined below, will be given with respect to a positive c_1. Except for the decays $\omega \to \eta\gamma$ and $\phi \to \eta'\gamma$, the theoretical partial decay widths are smaller than the experimental ones. Furthermore, we note that only for the decay $\omega \to \eta\gamma$ we find a deviation $|\delta_2|$ which is smaller than one. Using the experimental uncertainties, we obtain for the reduced chi-squared,

$$\chi^2_{\text{red}} = \frac{1}{\nu}\sum_{i=1}^{11} \frac{(\Gamma_i^{\text{exp}} - \Gamma_i^{\text{LO}})^2}{\sigma_i^2} = 94.,$$

where, omitting $\phi \to \pi^0\gamma$, the number of degrees of freedom is $\nu = 11 - 1 = 10$ at leading order. We conclude that a description in terms of a single coupling constant c_1 does not provide a good description of the twelve decays.

B. $1/N_c$ corrections

In the next scenario, we consider the $1/N_c$ corrections, but still stick to the SU(3) symmetry of the interaction terms. For the $\phi - \omega$ mixing we still take ideal mixing. Using $\bar{M}^2 = M_K^2 = M_\pi^2$ in the SU(3)-symmetric case, we find from Eq. (A5) of the Appendix that the quark-mass corrections simply result in a shift of the coupling constant c_1 of the leading-order Lagrangian, i.e., $c_1 \to \tilde{c}_1 = c_1 + 2\bar{M}^2 c_+$. On the other hand, the $1/N_c$ corrections (see Table XIV of the Appendix) affect both the $\rho^0\eta_1$ and $\omega_8\eta_1$ transitions in terms of the replacement $\tilde{c}_1 \to \tilde{c}_1 + \frac{3}{2}c_3$ and, similarly, both the $\pi^0\omega_1$ and $\eta_8\omega_1$ transitions in terms of the replacement $\tilde{c}_1 \to \tilde{c}_1 + \frac{3}{2}c_2$. The results of the fit for the SU(3)-symmetric case are shown in Table IV. The reduced chi-squared is now 45. (for twelve decays and 9 degrees of freedom) in comparison with 94. of the LO fit. The effective coupling constant $\tilde{c}_1$ comes out as $\tilde{c}_1 = (3.36 \pm 0.20) \times 10^{-2}$. Therefore, the decay rates for $\rho \to \pi\gamma$ and $K^* \to K\gamma$, which are not affected by c_2 and c_3, are reduced by the factor $(\tilde{c}_1/c_1)^2 = 0.77$. For the other decays, the situation is more complex. Even though the

TABLE IV. Decay rates including $1/N_c$ corrections in the SU(3)-symmetric case. For the experimental values, see Table III.

Decay	$\Gamma_{\text{LO}+1/N_c}$ (keV)	Deviation δ_1	Deviation δ_2
$\rho^0 \to \pi^0\gamma$	31.6 ± 3.7	-0.55	-3.1
$\rho^\pm \to \pi^\pm\gamma$	31.3 ± 3.7	-0.53	-4.3
$\rho^0 \to \eta\gamma$	23.2 ± 3.2	-0.48	-4.8
$\omega \to \pi^0\gamma$	$400. \pm 35.$	-0.45	-7.6
$\omega \to \eta\gamma$	5.64 ± 0.63	0.44	2.4
$\phi \to \pi^0\gamma$	5.4 ± 1.7	-0.039	-0.13
$\phi \to \eta\gamma$	59.1 ± 6.1	0.066	0.59
$\phi \to \eta'\gamma$	0.298 ± 0.056	0.13	0.60
$K^{*0} \to K^0\gamma$	70.5 ± 8.4	-0.39	-3.5
$K^{*\pm} \to K^\pm\gamma$	17.6 ± 2.1	-0.65	-6.4
$\eta' \to \rho^0\gamma$	46.5 ± 4.1	-0.16	-2.0
$\eta' \to \omega\gamma$	5.44 ± 0.67	0.15	1.0

TABLE V. Decay rates including $1/N_c$ and quark-mass corrections for $\Lambda_1 = -1/3, 0, 1/3$. For the mixing angles we made use of the NLO values $\theta_V = 39.8°$ and $\theta_P^{[1]} = -12.4°$.

Decay	Γ_{exp} (keV)	Γ (keV), $\Lambda_1 = -\frac{1}{3}$	Γ (keV), $\Lambda_1 = 0$	Γ (keV), $\Lambda_1 = \frac{1}{3}$
$\rho^0 \to \pi^0\gamma$	$70. \pm 12.$	$32. \pm 12.$	52.4 ± 9.8	71.5 ± 6.4
$\rho^\pm \to \pi^\pm\gamma$	67.1 ± 7.5	$32. \pm 12.$	52.0 ± 9.7	71.0 ± 6.4
$\rho^0 \to \eta\gamma$	44.7 ± 3.1	21.4 ± 8.0	37.4 ± 6.3	54.2 ± 4.1
$\omega \to \pi^0\gamma$	$723. \pm 25.$	$299. \pm 87.$	$459. \pm 69.$	$610. \pm 46.$
$\omega \to \eta\gamma$	3.91 ± 0.35	1.95 ± 0.63	3.32 ± 0.50	4.64 ± 0.33
$\phi \to \pi^0\gamma$	5.61 ± 0.26	4.5 ± 2.3	5.0 ± 1.4	5.65 ± 0.77
$\phi \to \eta\gamma$	55.4 ± 1.1	52.0 ± 9.7	53.9 ± 6.0	56.1 ± 3.3
$\phi \to \eta'\gamma$	0.2643 ± 0.0090	0.26 ± 0.82	0.258 ± 0.050	0.254 ± 0.027
$K^{*0} \to K^0\gamma$	$116. \pm 10.$	$86. \pm 16.$	$111. \pm 11.$	135.7 ± 6.9
$K^{*\pm} \to K^\pm\gamma$	50.4 ± 4.7	$50. \pm 43.$	$50. \pm 26.$	$50. \pm 14.$
$\eta' \to \rho^0\gamma$	55.5 ± 1.9	70.1 ± 9.1	62.0 ± 4.7	48.1 ± 2.0
$\eta' \to \omega\gamma$	4.74 ± 0.20	6.6 ± 1.3	6.48 ± 0.72	5.40 ± 0.30
χ^2_{red}	…	84.	32.	9.4

transitions $\omega_8 \to \eta_8\gamma$, $\omega_1 \to \eta_1\gamma$, $\rho^0 \to \eta_8\gamma$, and $\omega_8 \to \pi^0\gamma$ are still described in terms of $\tilde{c}_1$, because of the mixing of Eqs. (28) and (29), all of the remaining physical decays beyond $\rho \to \pi\gamma$ and $K^* \to K\gamma$ contain $\tilde{c}_1$ as well as $c_2 = (0.67 \pm 0.10) \times 10^{-2}$ and $c_3 = (-0.39 \pm 0.25) \times 10^{-2}$.

C. $1/N_c$ and quark-mass corrections

SU(3) symmetry implies that the amplitudes $\mathcal{A}$ of the decays $\rho \to \pi\gamma$, $K^{*\pm} \to K^\pm\gamma$, and $K^{*0} \to K^0\gamma$ satisfy the relations $|\mathcal{A}_{\rho\to\pi\gamma}| = |\mathcal{A}_{K^{*\pm}\to K^\pm\gamma}|$ and $|\mathcal{A}_{K^{*0}\to K^0\gamma}| = 2|\mathcal{A}_{K^{*\pm}\to K^\pm\gamma}|$ [57,58] (see also Table XIV). Using Eq. (39) together with the physical masses of Table I and the experimental decay rates of Table III, one obtains $|\mathcal{A}_{\rho^\pm\to\pi\gamma}|/|\mathcal{A}_{K^{*\pm}\to K^\pm\gamma}| = 0.909$ and $|\mathcal{A}_{K^{*0}\to K^0\gamma}|/|\mathcal{A}_{K^{*\pm}\to K^\pm\gamma}| = 1.59$, amounting, at the amplitude level, to an SU(3)-symmetry breaking of about 9% and 20%, respectively. This is of the same order of magnitude as the relative difference between the decay constants F_π and F_K, $(F_K - F_\pi)/F_K = 16\%$. The experimental decay rates for $\omega \to \pi^0\gamma$ and $\rho^0 \to \pi^0\gamma$ result in $|\mathcal{A}_{\omega\to\pi^0\gamma}|/|\mathcal{A}_{\rho^0\to\pi^0\gamma}| = 2.88$, very close to 3, the leading-order large-N_c prediction.

In the next step, we include the SU(3)-symmetry-breaking terms. With regard to the vector mesons, we now have to consider the $\phi - \omega$ mixing at next-to-leading order with a mixing angle of $\theta_V = 39.8°$.[8] For the decays involving pions and kaons, we need to take the wave function renormalization constants of Eqs. (27) into account. In terms of the pion and kaon decay constants of Eqs. (35), this amounts to replacing in the leading-order Lagrangian of Eq. (20) the decay constant F by the physical F_π and F_K in the corresponding cases. With reference to the Lagrangians of Eqs. (22) and (26) such replacement is of higher order. For the decays that involve an η or η', the situation is more complicated because of the mixing. Here, we make use of Eqs. (28) in combination with the NLO mixing angle $\theta_P^{[1]} = -12.4°$. Equations (28) introduce one additional, so far unspecified LEC of order $1/N_c$, namely, Λ_1, originating from the NLO kinetic Lagrangian of Eq. (8). We performed three fits with $\Lambda_1 = -1/3, 0, 1/3$, yielding the results shown in Table V.

Since the results turned out to be highly dependent on the value of the Λ_1 parameter, we performed fits that included Λ_1 as a free parameter in addition to the c_i parameters. In this context, we also consider two different scenarios: in the first case (denoted by I) we calculate the amplitude up to and including NLO and fit its square, whereas in the second case (II) we fit the squared amplitude only up to and including NLO. In other words, in the second case we do not keep terms of the order NNLO = NLO × NLO in the decay rate. Omitting for notational convenience the summation or averaging over the spins, we thus consider[9]

(i) $|\mathcal{M}^{\text{I}}|^2 = |\mathcal{M}_{\text{LO}}|^2 + 2\text{Re}(\mathcal{M}_{\text{LO}}\mathcal{M}^*_{\text{NLO}}) + |\mathcal{M}_{\text{NLO}}|^2$,
(ii) $|\mathcal{M}^{\text{II}}|^2 = |\mathcal{M}_{\text{LO}}|^2 + 2\text{Re}(\mathcal{M}_{\text{LO}}\mathcal{M}^*_{\text{NLO}})$.

The results for the two fits are shown in Table VI. Judging from the value of the reduced chi-squared, $\chi^2_{\text{red}} = 6.1$, we conclude that the second method provides the best description of the data. The corresponding set of parameters is given by

$$\begin{aligned} &c_1 = 0.0522 \pm 0.0020, \qquad c_2 = -0.00100 \pm 0.00021, \\ &c_3 = 0.00272 \pm 0.00072, \\ &c_+ = (2.80 \pm 0.78) \cdot 10^{-9}\ \text{MeV}^{-2}, \\ &c_- = (-6,1 \pm 43.9) \cdot 10^{-9}\ \text{MeV}^{-2}, \\ &\Lambda_1 = 0.290 \pm 0.050. \end{aligned} \tag{41}$$

[8]Since we did not take any corrections to the kinetic term into account, the wave function renormalization constants are still 1 for the vector mesons.

[9]Our previous results thus correspond to the first case.

TABLE VI. Decay rates using the two scenarios described in the text. In both cases Λ_1 is treated as a fit parameter. For the mixing angles we made use of the NLO values $\theta_V = 39.8°$ and $\theta_P^{[1]} = -12.4°$.

Decay	Γ_{PDG} (keV)	Γ^{I} (keV)	Γ^{II} (keV)
$\rho^0 \to \pi^0\gamma$	$70. \pm 12.$	70.3 ± 7.5	74.8 ± 5.7
$\rho^\pm \to \pi^\pm\gamma$	67.1 ± 7.5	69.8 ± 7.5	74.2 ± 5.7
$\rho^0 \to \eta\gamma$	44.7 ± 3.1	53.0 ± 5.5	51.9 ± 3.7
$\omega \to \pi^0\gamma$	$723. \pm 25.$	$601. \pm 55.$	$640. \pm 44.$
$\omega \to \eta\gamma$	3.91 ± 0.35	4.53 ± 0.46	4.31 ± 0.28
$\phi \to \pi^0\gamma$	5.61 ± 0.26	5.61 ± 0.84	5.65 ± 0.64
$\phi \to \eta\gamma$	55.4 ± 1.1	56.0 ± 3.6	55.7 ± 2.7
$\phi \to \eta'\gamma$	0.2643 ± 0.0090	0.255 ± 0.029	0.265 ± 0.022
$K^{*0} \to K^0\gamma$	$116. \pm 10.$	133.8 ± 8.8	128.3 ± 7.2
$K^{*\pm} \to K^\pm\gamma$	50.4 ± 4.6	$50. \pm 15.$	$50. \pm 12.$
$\eta' \to \rho^0\gamma$	55.5 ± 1.9	49.4 ± 4.2	49.6 ± 3.0
$\eta' \to \omega\gamma$	4.74 ± 0.20	5.52 ± 0.48	5.26 ± 0.39
χ^2_{red}	…	9.2	6.1
Λ_1	…	0.307 ± 0.074	0.290 ± 0.050

In Fig. 1, we present a visual comparison of the decay rates at leading order (red, middle entries) and at next-to-leading order in scenario II (blue, lower entries) with the experimental results (black, upper entries). Here, a clear improvement in the description of the decay rates can be seen in the transition from LO to NLO. To enable a quantitative comparison, we also show the deviations δ_1 and δ_2 of Eqs. (40) for our best-fit results in Table VII. Since our calculation is valid up to and including order $1/N_c$ and order χ, we expect uncertainties of the order of $\sqrt{(1/N_c)^4 + (\mathring{M}_K/(4\pi F))^8}$. Inserting $N_c = 3$ and the values of Table II for $\mathring{M}_K$ and F, this amounts to relative deviations of the order of 12%. After inspecting the column "deviation δ_1" of Table VII, we find that the relative deviation for almost all decays is more or less within this deviation. A notable exception is the decay $\rho^0 \to \eta\gamma$ with $\delta_1 = 16\%$. The deviations $\delta_2 = 1.5$, $\delta_2 = -1.6$, and $\delta_2 = -1.7$ for the decays $\rho^0 \to \eta\gamma$, $\omega \to \pi^0\gamma$, and $\eta' \to \rho^0\gamma$, respectively, hint at some tension, which will be partially resolved after refining the model. The linear combination $c_- = c_5 - c_6 - c_8$ only enters the charged decay $K^{*\pm} \to K^\pm\gamma$ (see Table XIV of the Appendix). Therefore, the central values of the experiment and of the fit coincide. As a consequence, the remaining linear combination, $c_+ = c_5 + c_6 - c_7$, is essentially the only parameter available to describe SU(3)-symmetry-breaking effects.

In Table VIII, we present the correlation coefficients $\langle \delta c_i \delta c_j \rangle / (\delta c_i \delta c_j)$ for our best fit of Table VII. As one might expect, the strongest correlation exists between parameters c_1 and c_+, because the linear combination $\tilde{c}_1 = c_1 + 2M_\pi^2 c_+$ contributes to all decays. There is also an equally strong correlation between c_1 and c_2.

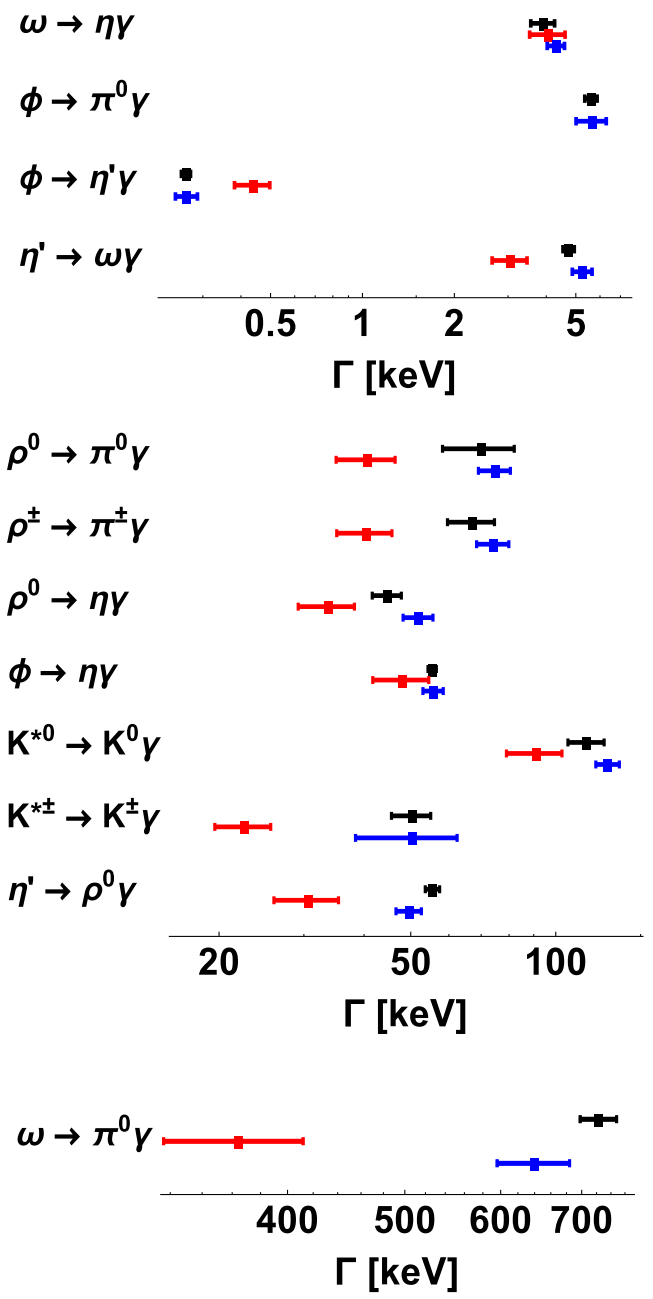

FIG. 1. Comparison of the decay rates at leading order (red, middle entries) and at next-to-leading order in scenario II (blue, lower entries) with the experimental results (black, upper entries).

The parameter c_2 only contributes to the transitions between the vector-meson singlet and the pseudoscalar-meson octet. There is a slightly smaller correlation between c_2 and c_+. Finally, the last notable correlations exist between the parameter Λ_1, which is of order $1/N_c$, and the parameters c_1 and c_3. The remaining correlations are negligibly small.

D. Expansion of the quark-charge matrix in $1/N_c$

As our final example, we also include the expansion of the quark-charge matrix in $1/N_c$ [see Eq. (18)]. As a

TABLE VII. Decay rates using the second scenario described in the text together with the deviations δ_1 and δ_2 of Eqs. (40).

Decay	$\Gamma_{\rm PDG}$ (keV)	$\Gamma_{\rm NLO}$ (keV)	Deviation δ_1	Deviation δ_2
$\rho^0 \to \pi^0\gamma$	$70. \pm 12.$	74.8 ± 5.7	0.066	0.35
$\rho^\pm \to \pi^\pm\gamma$	67.1 ± 7.5	74.2 ± 5.7	0.11	0.76
$\rho^0 \to \eta\gamma$	44.7 ± 3.1	51.9 ± 3.7	0.16	1.5
$\omega \to \pi^0\gamma$	$723. \pm 25.$	$640. \pm 44.$	−0.11	−1.6
$\omega \to \eta\gamma$	3.91 ± 0.35	4.31 ± 0.28	0.10	0.89
$\phi \to \pi^0\gamma$	5.61 ± 0.26	5.65 ± 0.64	0.007	0.060
$\phi \to \eta\gamma$	55.4 ± 1.1	55.7 ± 2.7	0.005	0.093
$\phi \to \eta'\gamma$	0.2643 ± 0.0090	0.265 ± 0.022	−0.002	−0.017
$K^{*0} \to K^0\gamma$	$116. \pm 10.$	128.3 ± 7.2	0.11	1.0
$K^{*\pm} \to K^\pm\gamma$	50.4 ± 4.6	$50. \pm 12.$	…	…
$\eta' \to \rho^0\gamma$	55.5 ± 1.9	49.6 ± 3.0	−0.11	−1.7
$\eta' \to \omega\gamma$	4.74 ± 0.20	5.26 ± 0.39	0.11	1.2

TABLE VIII. Off-diagonal array containing the correlation coefficients $\langle \delta c_i \delta c_j \rangle / (\delta c_i \delta c_j)$ of the parameters c_i for the fit of Table VII.

c_2	−0.73				
c_3	0.033	0.14			
c_+	−0.78	0.46	0.16		
c_-	0.21	−0.16	0.020	−0.13	
Λ_1	0.50	−0.19	0.50	−0.29	0.11
	c_1	c_2	c_3	c_+	c_-

consequence of this expansion, also the c_4 interaction Lagrangian of Eq. (22) contributes to the invariant amplitudes (see Table XV of the Appendix). Using the expressions of Table XV of the Appendix and applying scenario II of Sec. IV C, we obtain the results shown in Table IX. In fact, this scenario provides us with one additional parameter and it is therefore not surprising that $\chi^2_{\rm red} = 2.8$ (5 degrees of freedom) is smaller than the corresponding value $\chi^2_{\rm red} = 6.6$ of Table VI. The parameters of the fit are given by

$$\begin{aligned} c_1 &= 0.0536 \pm 0.0013, \\ c_2 &= -0.000613 \pm 0.000078, \\ c_3 &= 0.00109 \pm 0.00027, \\ c_4 &= 0.00142 \pm 0.00055, \\ c_+ &= (1.05 \pm 0.45) \cdot 10^{-9}\ \text{MeV}^{-2}, \\ c_- &= (5.1 \pm 1.6) \cdot 10^{-9}\ \text{MeV}^{-2}, \\ \Lambda_1 &= 0.247 \pm 0.032. \end{aligned} \tag{42}$$

In Fig. 2, we present a visual comparison of the decay rates at NLO in scenario II (blue, middle entries) and at NLO including a quark-charge expansion (green, lower entries) with the experimental results (black, upper entries). Except

TABLE IX. Decay rates using the second scenario described in the text, including an expansion of the quark-charge matrix in $1/N_c$. For the mixing angles we made use of the NLO values $\theta_V = 39.8°$ and $\theta_P^{[1]} = -12.4°$. $\chi^2_{\rm red} = 2.8$ (5 degrees of freedom).

Decay	$\Gamma_{\rm PDG}$ (keV)	$\Gamma_{\rm mod}$ in keV	δ_1	δ_2
$\rho^0 \to \pi^0\gamma$	$70. \pm 12.$	65.5 ± 5.6	−0.066	−0.35
$\rho^\pm \to \pi^\pm\gamma$	67.1 ± 7.5	65.0 ± 5.6	−0.031	−0.23
$\rho^0 \to \eta\gamma$	44.7 ± 3.1	51.5 ± 2.4	0.15	1.7
$\omega \to \pi^0\gamma$	$723. \pm 25.$	$689. \pm 30.$	−0.047	−0.87
$\omega \to \eta\gamma$	3.91 ± 0.35	3.80 ± 0.44	−0.028	−0.19
$\phi \to \pi^0\gamma$	5.61 ± 0.26	5.69 ± 0.43	0.014	0.16
$\phi \to \eta\gamma$	55.4 ± 1.1	55.0 ± 1.8	−0.0070	−0.18
$\phi \to \eta'\gamma$	0.2643 ± 0.0090	0.266 ± 0.015	0.0058	0.090
$K^{*0} \to K^0\gamma$	$116. \pm 10.$	138.6 ± 5.2	0.19	2.0
$K^{*\pm} \to K^\pm\gamma$	50.4 ± 4.6	50.4 ± 7.9	…	…
$\eta' \to \rho^0\gamma$	55.5 ± 1.9	53.4 ± 2.4	−0.038	−0.69
$\eta' \to \omega\gamma$	4.74 ± 0.20	4.87 ± 0.31	0.027	0.34

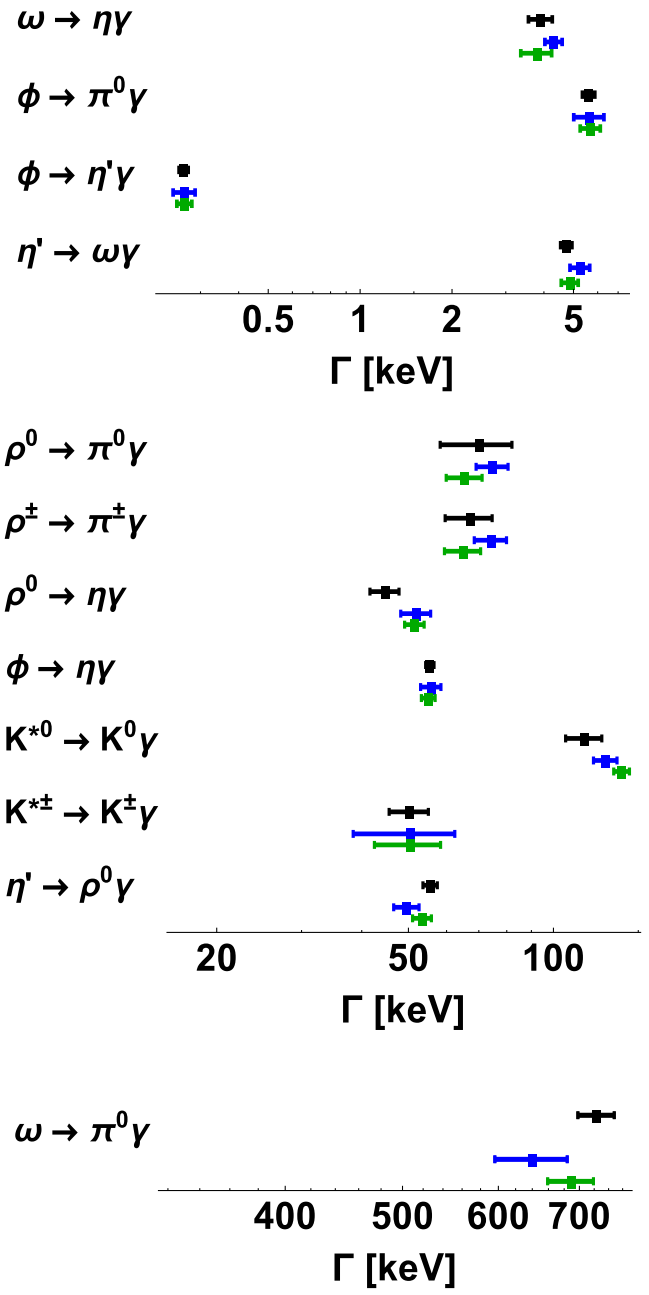

FIG. 2. Comparison of the decay rates at next-to-leading order in scenario II (blue, middle entries), next-to-leading order including a $1/N_c$ expansion of the quark-charge matrix (green, lower entries) with the experimental results (black, upper entries).

for the decays $\rho^0 \to \eta\gamma$ and $K^{*0} \to K^0\gamma$, we obtain an excellent agreement between experiment and theory.

E. Coupling constants and convergence

We have organized the Lagrangians in terms of $1/N_c$ and the quark masses m (contained in the quantities $\chi_\pm$). For the number of colors we insert $N_c = 3$ and, with respect to the quark-mass expansion, we consider $M_K^2/(4\pi F)^2 \approx 1/4$ as a typical small dimensionless expansion parameter, where $\Lambda_\chi = 4\pi F$ denotes the chiral-symmetry-breaking scale [91]. In Table X, we collect the coupling constants as obtained from fitting the data using different levels of approximation. The second column (LO) refers to the leading-order Lagrangian with $\theta_P = \theta_P^{[0]} = -19.7°$ and ideal $\phi - \omega$ mixing, the third column (LO+$1/N_c$) to the leading-order Lagrangian plus $1/N_c$ corrections with $\theta_P = \theta_P^{[0]} = -19.7°$ and ideal $\phi - \omega$ mixing, the fourth column to the complete next-to-leading-order Lagrangian without expanding the quark-charge matrix Q (NLO), and the fifth column to the complete next-to-leading-order Lagrangian including an expansion of Q (NLO, Q expanded). The last two scenarios made use of $\theta_P = \theta_P^{[1]} = -12.4°$, $\theta_V = 39.8°$, and physical values for F_π and F_K. As can be seen by comparing Tables XIV and XV of the Appendix, the contributions of the coefficients c_i to the decay matrix elements are redistributed in the version including the expansion of the quark-charge matrix. This is then the reason why, except for c_1, the coefficients differ notably for the last two cases.

Finally, we would like to comment on the order of magnitude of the corrections in comparison with the leading-order term. We multiply the constants c_2, c_3, and c_4 by a factor of 3 to obtain the coefficients belonging to the $1/N_c$ expansion. Similarly, we multiply c_+ and c_- by $(4\pi F)^2$ to obtain the coefficients for the dimensionless quark-mass expansion. The results corresponding to the last two columns of Table X are shown in Table XI. Let us have a closer look at the implications of the second column of Table XI (NLO with physical quark-charge matrix Q). We notice that all of the amplitudes $\mathcal{A}_i$ of Eq. (A2) except for $\mathcal{A}_5$ start with c_1. We multiply each $\mathcal{A}_i$ ($i \neq 5$) with a suitable factor such that the leading-order term is simply given by c_1. We can then easily identify the amount of the largest relative correction. Regarding the $1/N_c$ terms, this is $3c_2/(2c_1)$ for the amplitudes $\mathcal{A}_9$ and $\mathcal{A}_{11}$ and $3c_3/(2c_1)$ for the amplitudes $\mathcal{A}_7$ and $\mathcal{A}_{10}$, respectively. Using the values of the second column of Table XI, we obtain -0.086 and 0.23, respectively, where we have neglected the uncertainties. Keeping in mind that these numbers still have to be multiplied by $1/3$, the $1/N_c$ corrections turn out to be relatively small, namely -2.9% and 7.8%, respectively. For the quark-mass corrections, the largest correction originating from c_+ is found in the $\mathcal{A}_4$ amplitude, namely, the ratio $16|c_+|(4\pi F)^2/(3c_1) = 0.37$ which gets multiplied by $(M_K^2 - M_\pi^2)/(4\pi F)^2 = 0.17$. The relative quark-mass correction of 6.3% is of a similar magnitude as the $1/N_c$ correction. More pronounced is the case of the c_- coupling, resulting in the ratio $6|c_-|(4\pi F)^2/c_1 = 0.90$ which, together with the factor $(M_K^2 - M_\pi^2)/(4\pi F)^2 = 0.17$, gives rise to a relative correction of 15%. Recall that this parameter is entirely determined by the decay $K^{*\pm} \to K^\pm\gamma$. For the third column of Table XI (NLO with expanded quark-charge matrix Q), we obtain similar results.

TABLE X. Coupling constants determined at leading order (LO), leading order plus $1/N_c$ corrections, next-to-leading order (NLO), and next-to-leading order with expanded quark-charge matrix (NLO, Q expanded). See text for details.

Coupling constant	LO	LO + $1/N_c$	NLO	NLO, Q expanded
c_1 $[10^{-2}]$	3.82 ± 0.25	3.36 ± 0.20	5.22 ± 0.20	5.36 ± 0.13
c_2 $[10^{-2}]$	…	0.67 ± 0.10	-0.100 ± 0.021	-0.0613 ± 0.0078
c_3 $[10^{-2}]$	…	-0.39 ± 0.25	0.272 ± 0.072	0.109 ± 0.027
c_4 $[10^{-2}]$	…	…	…	0.142 ± 0.055
c_+ $[10^{-2}\ \mathrm{GeV}^{-2}]$	…	…	0.280 ± 0.078	0.105 ± 0.045
c_- $[10^{-2}\ \mathrm{GeV}^{-2}]$	…	…	-0.61 ± 0.39	0.51 ± 0.16

TABLE XI. Expansion coefficients at next-to-leading order (NLO) corresponding to the last two columns of Table X. For simplicity we suppress uncertainties.

Coefficients	Physical Q	Q expanded
$\tilde{c}_1$ $[10^{-2}]$	5.23	5.36
$c_2 \cdot N_c$ $[10^{-2}]$	−0.30	−0.18
$c_3 \cdot N_c$ $[10^{-2}]$	0.82	0.33
$c_4 \cdot N_c$ $[10^{-2}]$	…	0.43
$c_+ \cdot (4\pi F)^2$ $[10^{-2}]$	0.36	0.14
$c_- \cdot (4\pi F)^2$ $[10^{-2}]$	−0.79	0.67

F. Corrections beyond the tree level

Our results represent a phenomenological treatment of $1/N_c$ and quark-mass corrections beyond the simplest tree-level calculation (with only one single coupling constant). Clearly, a more ambitious perturbative method that has a higher claim than pure phenomenology requires the consideration of quantum corrections at least at the one-loop level. In a first step, it seems obvious to first consider purely pseudoscalar loop corrections which we expect to give rise to terms proportional to M^2 and $M^2 \ln(M^2/\mu^2)$, where M denotes a pseudoscalar meson mass. The dependence on the renormalization scale μ should be cancelled by corresponding counterterms. With respect to implementing a viable power counting scheme, which, in addition, also accounts for internal vector-meson lines, one could try to either make use of the heavy-vector-meson formulation [37,92,93] or apply the complex-mass scheme of Ref. [36,94].

G. Comparison with other calculations in chiral effective Lagrangian approaches

Reference [64] contains the leading-order Lagrangian of the vector formulation for the $VP\gamma$ decay of neutral vector mesons into neutral pions. When comparing this with Eq. (3.19) of Ref. [64], we agree after identifying our $2ec_1/F$ with d/f_π of Ref. [64].[10] However, their Eq. (4.7) for the decay rates seems to contain an error, namely, the second line needs to be multiplied by a factor of $1/9$, originating from the elements of the quark-charge matrix in the form $(2/3 - 1/3)^2$. Accordingly, the coupling $d \simeq 0.01$ of Eq. (4.10) needs to be multiplied by a factor of 3. Similarly, our results from the leading-order Lagrangian agree with the coefficients reported in Fig. 3 of Ref. [61], which, beyond SU(3) symmetry, implicitly made use of nonet symmetry in combination with ideal $\phi - \omega$ mixing and neglected $\eta - \eta'$ mixing.

In Ref. [93], the heavy-vector-meson approach of Ref. [92] was applied to processes with a net disappearance of vector mesons. The lowest-order odd-intrinsic-parity Lagrangian of Ref. [93] (see Eq. (22) of [93]) gives rise to the same results as our leading-order interaction Lagrangian of Eq. (17). Next-to-leading-order corrections were not considered in Ref. [93].

The antisymmetric tensor-field representation [54,55] was used in, e.g., Refs. [35,66–68] for the calculation of the $VP\gamma$ interaction. In Ref. [66], the relevant interaction Lagrangian for the interaction of two vector fields with one pseudoscalar field (VVP) and for one vector resonance with an external vector field and a pseudoscalar field (VJP) was constructed, involving $7 + 4$ coupling constants, respectively. In terms of the QCD short-distance behavior of the VVP Green function, constraints among the coupling constants were derived. Using these constraints, Eq. (4.2) of Ref. [66] provides a parameter-free prediction for the $\omega \to \pi^0\gamma$-transition matrix element, translating into a prediction for our c_1,

$$|c_1| = \frac{1}{4\sqrt{2}}\left(\frac{3}{8\pi^2}\frac{m_\omega}{F} - \frac{F}{2}\frac{m_\omega}{m_V^2}\right).$$

Using $F = 90.9$ MeV and $m_\omega = m_V = 782.7$ MeV, one obtains $|c_1| = 4.76 \times 10^{-2}$ which has to be compared with our LO prediction $|c_1| = (3.82 \pm 0.25) \times 10^{-2}$ and the NLO prediction $|c_1| = (5.22 \pm 0.20) \times 10^{-2}$ of Table X. In Ref. [35], antisymmetric tensor fields were used for describing the radiative decays of the vector-meson nonet into the pseudoscalar octet. The η' was not considered, the physical η was taken as part of the pseudoscalar octet, and for the $\phi - \omega$

[10]Note that the vector-meson matrix of Ref. [64] is two times our vector-meson matrix.

system an ideal mixing was assumed. The decay proceeds either via a VVP vertex such that the propagating neutral vector meson subsequently couples to a real photon or via a direct $VP\gamma$ interaction (which is considered to be of higher order in their chiral counting). The decay rates then contain three (combinations of) coupling constants, namely e_A (direct decay), $h_A e_V$ and $b_A e_V$ (indirect decay) (see Eqs. (38)–(42) of Ref. [35]). In the limit of SU(3) symmetry, our results for the invariant amplitudes fully agree with those of Ref. [35]. To see this, one needs to set all vector-meson masses equal to m_V, all pseudoscalar meson masses equal to $\bar{M}$, $F = f$, and, finally, $e|\tilde{c}_1| = |\tilde{e}_A|/8$, where $\tilde{e}_A = e_A + \frac{1}{4} h_A e_V - 2 b_A e_V \bar{M}^2/m_V^2$. In Ref. [67], the analysis was extended to also include the η' meson. With two additional parameters, namely, the $\eta - \eta'$ mixing angle θ_P and one parameter b_H for the interaction of the singlet eta with two vector mesons, in total five parameters were adjusted to five decays. In particular, an unconventionally small mixing angle $\theta_P \simeq \pm 2°$ was found. When taking SU(3)-symmetry breaking effects into account, in our framework two additional parameters are available, namely, c_+ and c_-, whereas in the framework of Ref. [35] only the combination $b_A e_V$ will give rise to SU(3)-symmetry breaking effects. This term corresponds to our c_+ structure. In particular, the SU(3) relation $|\mathcal{A}_{K^{*0}\to K^0\gamma}| = 2|\mathcal{A}_{K^{*\pm}\to K^\pm\gamma}|$ will not be broken in the framework of Ref. [35], unless higher-order terms are taken into account. In our calculation, the parameter c_- decouples $\mathcal{A}_{K^{*\pm}\to K^\pm\gamma}$ and $\mathcal{A}_{K^{*0}\to K^0\gamma}$. On the other hand, in Ref. [68], the importance of such a term in the context of SU(3) symmetry breaking was already worked out for the radiative $K^* \to K\gamma$ decays. Reference [68] extended the results of [66] by also including excited vector-meson resonances.

Recently, Kimura, Morozumi, and Umeeda [69] investigated decays of light hadrons within a chiral Lagrangian model that includes both the lightest pseudoscalar and vector mesons. As an extension of chiral perturbation theory, they included one-loop corrections due to the Goldstone bosons and the corresponding counterterms. In addition to other processes, they also particularly looked at the $VP\gamma$ reactions. For the decays involving the light vector mesons, the model provides three parameters.

In Table XII, we provide a comparison of our results with those of Ref. [69]. First of all, we note that, with the exception of the decays $\omega \to \pi^0\gamma$ and $K^{*0} \to K^0\gamma$, our central values for the decay rates agree better with the experimental values than those from Ref. [69]. In addition, the uncertainties from Ref. [69] are, on average, much larger than ours. We conclude that our approach provides an improved description of the $VP\gamma$ decays.

TABLE XII. Comparison of our results at NLO with the predictions of Ref. [69] (KMU18).

Decay	Γ_{exp} [keV]	Γ_{NLO} [keV]	Γ_{KMU18} [keV]
$\rho^0 \to \pi^0\gamma$	$70. \pm 12.$	65.5 ± 5.6	$46. \pm 5.$
$\rho^\pm \to \pi^\pm\gamma$	67.1 ± 7.5	65.0 ± 5.6	$73. \pm 7.$
$\rho^0 \to \eta\gamma$	44.7 ± 3.1	51.5 ± 2.4	$33.^{+8.}_{-9.}$
$\omega \to \pi^0\gamma$	$723. \pm 25.$	$689. \pm 30.$	$710. \pm 90.$
$\omega \to \eta\gamma$	3.91 ± 0.35	3.80 ± 0.44	$5.5^{+1.6}_{-1.3}$
$\phi \to \pi^0\gamma$	5.61 ± 0.26	5.69 ± 0.43	$17.^{+12.}_{-9.}$
$\phi \to \eta\gamma$	55.4 ± 1.1	55.0 ± 1.8	$22.^{+9.}_{-12.}$
$\phi \to \eta'\gamma$	0.2643 ± 0.0090	0.266 ± 0.015	$0.39^{+0.12}_{-0.09}$
$K^{*0} \to K^0\gamma$	$116. \pm 10.$	138.6 ± 5.2	$110. \pm 10.$
$K^{*\pm} \to K^\pm\gamma$	50.4 ± 4.6	50.4 ± 7.9	$28. \pm 3.$
$\eta' \to \rho^0\gamma$	55.5 ± 1.9	53.4 ± 2.4	…
$\eta' \to \omega\gamma$	4.74 ± 0.20	4.87 ± 0.31	$4.6^{+3.3}_{-2.0}$

V. SUMMARY

In this work we analyzed the radiative transitions between the vector-meson nonet and the pseudoscalar-meson nonet within a chiral effective Lagrangian approach. For that purpose we have determined the Lagrangian up to and including the next-to-leading order in an expansion in $1/N_c$ and the quark masses. For the transformation behavior of the vector mesons under the Lorentz group we made use of the vector representation. At leading order, the Lagrangian contains one free parameter which was determined from a simultaneous fit to 11 experimental decay rates. (The decay $\phi \to \pi^0\gamma$ was excluded because of the OZI rule.) Both $\eta - \eta'$ and $\phi - \omega$ mixing were taken into account at leading order. The results of this scenario are given in Table III and clearly show that a good description of all experimental data at leading order is not possible. We then gradually improved the model by first taking into account $1/N_c$ corrections (see Table IV) and then also quark mass corrections (see Table V), which introduced 2 plus 2 additional parameters, respectively. In this context, we also had to consider the corrections due to the wave function renormalization and the mixing at NLO. As a result, another parameter of the $\eta - \eta'$ system was included in the calculation, which served as a further fit parameter. Then fits were carried out in which either the invariant amplitude or the decay were expanded up to and including next-to-leading order (scenario I and II, respectively). From Table VI we concluded that the second scenario yields a better description of the experimental data. In Fig. 2 we provided a visual presentation of the improvement from LO to NLO. However, one has to keep in mind in this context that at leading order only one free parameter is available to describe 11 decays, while at NLO 6 parameters (including Λ_1) have been fitted to 12 decays. In our final fit we made use of a $1/N_c$ expansion of the quark-charge matrix, which gives rise to one additional free parameter and results in the best description of the data (see Table IX and Fig. 2). We also found that the contributions to the amplitudes $\mathcal{A}_i$ of Eq. (A2), which are generated by the $1/N_c$ and the quark mass corrections, are smaller in magnitude than 15% of the leading-order term. In other

words, they can really be regarded as corrections. Clearly, our approach is limited in the sense that extending it to include even NNLO corrections would introduce a number of additional parameters such that there would be no more predictive power. However, it would be interesting to see how pseudoscalar-meson loop corrections affect our findings [95]. In summary, we can say that the present calculation is the most comprehensive investigation of the $VP\gamma$ decays to date and provides a satisfactory description of the experimental decay rates.

ACKNOWLEDGMENTS

Supported by the Deutsche Forschungsgemeinschaft DFG through the Collaborative Research Center "The Low-Energy Frontier of the Standard Model" (SFB 1044). The authors would like to thank Wolfgang Gradl for discussions of the experimental results.

APPENDIX: LAGRANGIANS

Let us introduce the following structures involving the singlet and octet fields:

$$\begin{aligned}
T_{1\rho\sigma} &= \rho_\rho^+\partial_\sigma\pi^- + \rho_\rho^-\partial_\sigma\pi^+ + \rho_\rho^0\partial_\sigma\pi^0,\\
T_{2\rho\sigma} &= K_\rho^{*+}\partial_\sigma K^- + K_\rho^{*-}\partial_\sigma K^+,\\
T_{3\rho\sigma} &= \bar{K}_\rho^{*0}\partial_\sigma K^0 + K_\rho^{*0}\partial_\sigma\bar{K}^0,\\
T_{4\rho\sigma} &= \omega_{8\rho}\partial_\sigma\eta_8,\\
T_{5\rho\sigma} &= \omega_{1\rho}\partial_\sigma\eta_1,\\
T_{6\rho\sigma} &= \rho_\rho^0\partial_\sigma\eta_8,\\
T_{7\rho\sigma} &= \rho_\rho^0\partial_\sigma\eta_1,\\
T_{8\rho\sigma} &= \omega_{8\rho}\partial_\sigma\pi^0,\\
T_{9\rho\sigma} &= \omega_{1\rho}\partial_\sigma\pi^0,\\
T_{10\rho\sigma} &= \omega_{8\rho}\partial_\sigma\eta_1,\\
T_{11\rho\sigma} &= \omega_{1\rho}\partial_\sigma\eta_8.
\end{aligned} \tag{A1}$$

The effective Lagrangian of the $VP\gamma$ interaction may then be written as

$$\mathcal{L}_{\text{eff}}^{VP\gamma} = e\epsilon^{\mu\nu\rho\sigma}F_{\mu\nu}\sum_{i=1}^{11}\mathcal{A}_i T_{i\rho\sigma}. \tag{A2}$$

TABLE XIII. Charge factors for physical values and the limit $N_c \to \infty$.

	Physical value	Value as $N_c \to \infty$
Q_u	$\frac{2}{3}$	$\frac{1}{2}$
Q_d	$-\frac{1}{3}$	$-\frac{1}{2}$
Q_s	$-\frac{1}{3}$	$-\frac{1}{2}$
Q_u+Q_d	$\frac{1}{3}$	0
Q_u+Q_s	$\frac{1}{3}$	0
Q_d+Q_s	$-\frac{2}{3}$	-1
Q_u-Q_d	1	1
$Q_u+Q_d+4Q_s$	-1	-2
$Q_u+Q_d-2Q_s$	1	1
$Q_u+Q_d+Q_s$	0	$-\frac{1}{2}$

Defining

$$\begin{aligned}
E^{\rho\sigma} &\equiv 2\frac{e}{F}\epsilon^{\rho\sigma\mu\nu}F_{\mu\nu},\\
H_{\rho\sigma} &\equiv \Big[(Q_u+Q_d)T_{1\rho\sigma}+(Q_u+Q_s)T_{2\rho\sigma}+(Q_d+Q_s)T_{3\rho\sigma}\\
&\quad+\frac{1}{3}(Q_u+Q_d+4Q_s)T_{4\rho\sigma}+\frac{2}{3}(Q_u+Q_d+Q_s)T_{5\rho\sigma}\\
&\quad+(Q_u-Q_d)\left(\frac{1}{\sqrt{3}}T_{6\rho\sigma}+\sqrt{\frac{2}{3}}T_{7\rho\sigma}+\frac{1}{\sqrt{3}}T_{8\rho\sigma}+\sqrt{\frac{2}{3}}T_{9\rho\sigma}\right)\\
&\quad+\frac{\sqrt{2}}{3}(Q_u+Q_d-2Q_s)(T_{10\rho\sigma}+T_{11\rho\sigma})\Big],
\end{aligned}$$

where Q_u, Q_d, and Q_s denote the quark charges, the Lagrangian of Eq. (20) is given by

$$\mathcal{L}_{\text{LO}}^{VP\gamma} = c_1 E^{\rho\sigma}H_{\rho\sigma}. \tag{A3}$$

The charge factors are given in Table XIII both for the physical charges and their values as $N_c \to \infty$. Note that the $T_{5\rho\sigma}$ term does not contribute for physical values of the quark charges.

The $1/N_c$ corrections are given by

$$\begin{aligned}
\mathcal{L}_{\text{NLO},1/N_c}^{VP\gamma} = E^{\rho\sigma}\Big\{&c_2\left[(Q_u+Q_d+Q_s)T_{5\rho\sigma}+\sqrt{\frac{3}{2}}(Q_u-Q_d)T_{9\rho\sigma}+\frac{1}{\sqrt{2}}(Q_u+Q_d-2Q_s)T_{11\rho\sigma}\right]\\
&+c_3\left[(Q_u+Q_d+Q_s)T_{5\rho\sigma}+\sqrt{\frac{3}{2}}(Q_u-Q_d)T_{7\rho\sigma}+\frac{1}{\sqrt{2}}(Q_u+Q_d-2Q_s)T_{10\rho\sigma}\right]\\
&+c_4(Q_u+Q_d+Q_s)(T_{1\rho\sigma}+T_{2\rho\sigma}+T_{3\rho\sigma}+T_{4\rho\sigma}+T_{5\rho\sigma})\Big\}.
\end{aligned} \tag{A4}$$

Since $\langle Q \rangle = Q_u + Q_d + Q_s = 0$ for the physical quark charges, the last term does not contribute in this case. Furthermore, for physical quark charges, there is no singlet-to-singlet transition ($T_{5\rho\sigma}$). In order to express the quark mass corrections we make use of the leading-order kaon and pion masses squared [15], $\overset{\circ}{M}{}_K^2 = B_0(\hat{m} + m_s)$ and $\overset{\circ}{M}{}_\pi^2 = 2B_0\hat{m}$. To the order we are considering, we replace the leading-order expressions by the physical values, i.e., $\overset{\circ}{M}{}_K^2 \to M_K^2$ and $\overset{\circ}{M}{}_\pi^2 \to M_\pi^2$. The quark-mass corrections are then given by

$$
\begin{aligned}
\mathcal{L}^{VP\gamma}_{\mathrm{NLO},\chi} = {} & (2c_5 - c_7 - c_8)E^{\rho\sigma}\Big\{ M_\pi^2(Q_u + Q_d)T_{1\rho\sigma} + [M_\pi^2 Q_u + (2M_K^2 - M_\pi^2)Q_s]T_{2\rho\sigma} \\
& + [M_\pi^2 Q_d + (2M_K^2 - M_\pi^2)Q_s]T_{3\rho\sigma} + \frac{1}{3}[M_\pi^2(Q_u + Q_d) + 4Q_s(2M_K^2 - M_\pi^2)]T_{4\rho\sigma} \\
& + \frac{2}{3}[M_\pi^2(Q_u + Q_d) + (2M_K^2 - M_\pi^2)Q_s]T_{5\rho\sigma} \\
& + M_\pi^2(Q_u - Q_d)\left(\frac{1}{\sqrt{3}}T_{6\rho\sigma} + \sqrt{\frac{2}{3}}T_{7\rho\sigma} + \frac{1}{\sqrt{3}}T_{8\rho\sigma} + \sqrt{\frac{2}{3}}T_{9\rho\sigma}\right) \\
& + \frac{\sqrt{2}}{3}[M_\pi^2(Q_u + Q_d) - 2(2M_K^2 - M_\pi^2)Q_s](T_{10\rho\sigma} + T_{11\rho\sigma})\Big\} \\
& + (2c_6 - c_7 + c_8)E^{\rho\sigma}\Big\{ M_\pi^2(Q_u + Q_d)T_{1\rho\sigma} + [(2M_K^2 - M_\pi^2)Q_u + M_\pi^2 Q_s]T_{2\rho\sigma} \\
& + [(2M_K^2 - M_\pi^2)Q_d + M_\pi^2 Q_s]T_{3\rho\sigma} + \frac{1}{3}[M_\pi^2(Q_u + Q_d) + 4Q_s(2M_K^2 - M_\pi^2)]T_{4\rho\sigma} \\
& + \frac{2}{3}[M_\pi^2(Q_u + Q_d) + (2M_K^2 - M_\pi^2)Q_s]T_{5\rho\sigma} \\
& + M_\pi^2(Q_u - Q_d)\left(\frac{1}{\sqrt{3}}T_{6\rho\sigma} + \sqrt{\frac{2}{3}}T_{7\rho\sigma} + \frac{1}{\sqrt{3}}T_{8\rho\sigma} + \sqrt{\frac{2}{3}}T_{9\rho\sigma}\right) \\
& + \frac{\sqrt{2}}{3}[M_\pi^2(Q_u + Q_d) - 2(2M_K^2 - M_\pi^2)Q_s](T_{10\rho\sigma} + T_{11\rho\sigma})\Big\}.
\end{aligned}
$$

Using $2M_K^2 - M_\pi^2 = M_\pi^2 + 2(M_K^2 - M_\pi^2)$ and noting that $Q_d = Q_s$, we may write

$$
\begin{aligned}
\mathcal{L}^{VP\gamma}_{\mathrm{NLO},\chi} = {} & 2M_\pi^2(c_5 + c_6 - c_7)E^{\rho\sigma}T_{\rho\sigma} \\
& + 4(M_K^2 - M_\pi^2)(c_5 + c_6 - c_7)E^{\rho\sigma}\left[\frac{1}{2}(Q_u + Q_s)T_{2\rho\sigma} + Q_s T_{3\rho\sigma} + \frac{4}{3}Q_s T_{4\rho\sigma} + \frac{2}{3}Q_s T_{5\rho\sigma} - 2\frac{\sqrt{2}}{3}Q_s(T_{10\rho\sigma} + T_{11\rho\sigma})\right] \\
& + 2(M_K^2 - M_\pi^2)(c_5 - c_6 - c_8)E^{\rho\sigma}(Q_s - Q_u)T_{2\rho\sigma}. \qquad \text{(A5)}
\end{aligned}
$$

In Table XIV, we collect the amplitudes $\mathcal{A}_i$, $i = 1, \ldots, 11$, of Eq. (A2). We have defined $c_+ = c_5 + c_6 - c_7$, $c_- = c_5 - c_6 - c_8$, and $\tilde{c}_1 = c_1 + 2M_\pi^2 c_+$. The results depend on 5 parameters c_1 ($\tilde{c}_1$), c_2, c_3, c_+, and c_-.

In Table XV, we collect the corresponding coefficients of the large-N_c expansion. We show the results at leading order (LO) and at next-to-leading order (NLO), depending on one parameter and six parameters, respectively.

TABLE XIV. Amplitudes $\mathcal{A}_i$ for the full result in units of $2/F$; $c_+ = c_5 + c_6 - c_7$, $c_- = c_5 - c_6 - c_8$, $\tilde{c}_1 = c_1 + 2M_\pi^2 c_+$.

Transition	Structure	Amplitude $\mathcal{A}_i$ in units of $2/F$
$\rho \to \pi\gamma$	T_1	$\frac{1}{3}\tilde{c}_1$
$K^{*\pm} \to K^\pm\gamma$	T_2	$\frac{1}{3}\tilde{c}_1 + \frac{2}{3}(M_K^2 - M_\pi^2)c_+ - 2(M_K^2 - M_\pi^2)c_-$
$K^* \to K^0\gamma$	T_3	$-\frac{2}{3}\tilde{c}_1 - \frac{4}{3}(M_K^2 - M_\pi^2)c_+$
$\omega_8 \to \eta_8\gamma$	T_4	$-\frac{1}{3}\tilde{c}_1 - \frac{16}{9}(M_K^2 - M_\pi^2)c_+$
$\omega_1 \to \eta_1\gamma$	T_5	$-\frac{8}{9}(M_K^2 - M_\pi^2)c_+$
$\rho^0 \to \eta_8\gamma$	T_6	$\frac{1}{\sqrt{3}}\tilde{c}_1$
$\rho^0 \to \eta_1\gamma$	T_7	$\sqrt{\frac{2}{3}}\tilde{c}_1 + \sqrt{\frac{3}{2}}c_3$
$\omega_8 \to \pi^0\gamma$	T_8	$\frac{1}{\sqrt{3}}\tilde{c}_1$
$\omega_1 \to \pi^0\gamma$	T_9	$\sqrt{\frac{2}{3}}\tilde{c}_1 + \sqrt{\frac{3}{2}}c_2$
$\omega_8 \to \eta_1\gamma$	T_{10}	$\frac{\sqrt{2}}{3}\tilde{c}_1 + \frac{1}{\sqrt{2}}c_3 + \frac{8\sqrt{2}}{9}(M_K^2 - M_\pi^2)c_+$
$\omega_1 \to \eta_8\gamma$	T_{11}	$\frac{\sqrt{2}}{3}\tilde{c}_1 + \frac{1}{\sqrt{2}}c_2 + \frac{8\sqrt{2}}{9}(M_K^2 - M_\pi^2)c_+$

TABLE XV. Amplitudes $\mathcal{A}_i$ in the large-N_c expansion in units of $2/F$; $c_+ = c_5 + c_6 - c_7$, $c_- = c_5 - c_6 - c_8$.

Structure	Amplitude $\mathcal{A}_i$ at LO in $[2/F]$	Amplitude $\mathcal{A}_i$ at NLO in $[2/F]$
T_1	0	$\frac{1}{3}c_1 - \frac{1}{2}c_4$
T_2	0	$\frac{1}{3}c_1 - \frac{1}{2}c_4 - 2(M_K^2 - M_\pi^2)c_-$
T_3	$-c_1$	$-\frac{2}{3}c_1 - \frac{1}{2}c_4 - 2M_K^2 c_+$
T_4	$-\frac{2}{3}c_1$	$-\frac{1}{3}c_1 - \frac{1}{2}c_4 - \frac{4}{3}(2M_K^2 - M_\pi^2)c_+$
T_5	$-\frac{1}{3}c_1$	$-\frac{1}{2}c_2 - \frac{1}{2}c_3 - \frac{1}{2}c_4 - \frac{2}{3}(2M_K^2 - M_\pi^2)c_+$
T_6	$\frac{1}{\sqrt{3}}c_1$	$\frac{1}{\sqrt{3}}c_1 + \frac{2}{\sqrt{3}}M_\pi^2 c_+$
T_7	$\sqrt{\frac{2}{3}}c_1$	$\sqrt{\frac{2}{3}}c_1 + \sqrt{\frac{3}{2}}c_3 + 2\sqrt{\frac{2}{3}}M_\pi^2 c_+$
T_8	$\frac{1}{\sqrt{3}}c_1$	$\frac{1}{\sqrt{3}}c_1 + \frac{2}{\sqrt{3}}M_\pi^2 c_+$
T_9	$\sqrt{\frac{2}{3}}c_1$	$\sqrt{\frac{2}{3}}c_1 + \sqrt{\frac{3}{2}}c_2 + 2\sqrt{\frac{2}{3}}M_\pi^2 c_+$
T_{10}	$\frac{\sqrt{2}}{3}c_1$	$\frac{\sqrt{2}}{3}c_1 + \frac{1}{\sqrt{2}}c_3 + \frac{2}{3}\sqrt{2}(2M_K^2 - M_\pi^2)c_+$
T_{11}	$\frac{\sqrt{2}}{3}c_1$	$\frac{\sqrt{2}}{3}c_1 + \frac{1}{\sqrt{2}}c_2 + \frac{2}{3}\sqrt{2}(2M_K^2 - M_\pi^2)c_+$

[1] J. Gasser and H. Leutwyler, Phys. Rep. **87**, 77 (1982).
[2] J. Goldstone, Nuovo Cimento **19**, 154 (1961).
[3] J. Goldstone, A. Salam, and S. Weinberg, Phys. Rev. **127**, 965 (1962).
[4] G. 't Hooft, Nucl. Phys. **B72**, 461 (1974).
[5] E. Witten, Nucl. Phys. **B160**, 57 (1979).
[6] P. Di Vecchia and G. Veneziano, Nucl. Phys. **B171**, 253 (1980).
[7] S. R. Coleman and E. Witten, Phys. Rev. Lett. **45**, 100 (1980).
[8] S. L. Adler, Phys. Rev. **177**, 2426 (1969).
[9] J. S. Bell and R. Jackiw, Nuovo Cimento A **60**, 47 (1969).
[10] G. 't Hooft, Phys. Rev. Lett. **37**, 8 (1976).
[11] E. Witten, Nucl. Phys. **B156**, 269 (1979).
[12] G. Veneziano, Nucl. Phys. **B159**, 213 (1979).
[13] S. Weinberg, Physica (Amsterdam) **96A**, 327 (1979).
[14] J. Gasser and H. Leutwyler, Ann. Phys. (N.Y.) **158**, 142 (1984).
[15] J. Gasser and H. Leutwyler, Nucl. Phys. **B250**, 465 (1985).
[16] J. F. Donoghue, E. Golowich, and B. R. Holstein, *Dynamics of the Standard Model* (Cambridge University Press, Cambridge, England, 1992).
[17] S. Scherer, Adv. Nucl. Phys. **27**, 277 (2003).
[18] S. Scherer and M. R. Schindler, Lect. Notes Phys. **830**, 1 (2012).
[19] B. Moussallam, Phys. Rev. D **51**, 4939 (1995).
[20] H. Leutwyler, Phys. Lett. B **374**, 163 (1996).
[21] P. Herrera-Siklody, J. I. Latorre, P. Pascual, and J. Taron, Nucl. Phys. **B497**, 345 (1997).
[22] R. Kaiser and H. Leutwyler, Eur. Phys. J. C **17**, 623 (2000).
[23] H. Leutwyler, Nucl. Phys. B, Proc. Suppl. **64**, 223 (1998).
[24] R. Kaiser and H. Leutwyler, in *Nonperturbative Methods in Quantum Field Theory* (World Scientific, Singapore, 1998).
[25] P. Herrera-Siklody, Phys. Lett. B **442**, 359 (1998).
[26] B. Borasoy, Eur. Phys. J. C **34**, 317 (2004).
[27] X. K. Guo, Z. H. Guo, J. A. Oller, and J. J. Sanz-Cillero, J. High Energy Phys. 06 (**2015**) 175.
[28] P. Bickert, P. Masjuan, and S. Scherer, Phys. Rev. D **95**, 054023 (2017).
[29] J. Gasser, M. E. Sainio, and A. Švarc, Nucl. Phys. **B307**, 779 (1988).
[30] E. E. Jenkins and A. V. Manohar, Phys. Lett. B **255**, 558 (1991).
[31] T. Becher and H. Leutwyler, Eur. Phys. J. C **9**, 643 (1999).
[32] J. Gegelia and G. Japaridze, Phys. Rev. D **60**, 114038 (1999).
[33] T. Fuchs, J. Gegelia, G. Japaridze, and S. Scherer, Phys. Rev. D **68**, 056005 (2003).
[34] P. C. Bruns and U.-G. Meissner, Eur. Phys. J. C **40**, 97 (2005).
[35] M. F. M. Lutz and S. Leupold, Nucl. Phys. **A813**, 96 (2008).
[36] D. Djukanovic, J. Gegelia, A. Keller, and S. Scherer, Phys. Lett. B **680**, 235 (2009).
[37] J. Bijnens, P. Gosdzinsky, and P. Talavera, J. High Energy Phys. 01 (1998) 014.
[38] S. Weinberg, Phys. Rev. **166**, 1568 (1968).
[39] S. R. Coleman, J. Wess, and B. Zumino, Phys. Rev. **177**, 2239 (1969).
[40] C. G. Callan, Jr., S. R. Coleman, J. Wess, and B. Zumino, Phys. Rev. **177**, 2247 (1969).
[41] O. Kaymakcalan, S. Rajeev, and J. Schechter, Phys. Rev. D **30**, 594 (1984).
[42] O. Kaymakcalan and J. Schechter, Phys. Rev. D **31**, 1109 (1985).
[43] M. Bando, T. Kugo, and K. Yamawaki, Nucl. Phys. **B259**, 493 (1985).

[44] U.-G. Meißner, Phys. Rep. **161**, 213 (1988).
[45] M. Bando, T. Kugo, and K. Yamawaki, Phys. Rep. **164**, 217 (1988).
[46] G. Ecker, J. Gasser, A. Pich, and E. de Rafael, Nucl. Phys. **B321**, 311 (1989).
[47] G. Ecker, J. Gasser, H. Leutwyler, A. Pich, and E. de Rafael, Phys. Lett. B **223**, 425 (1989).
[48] M. C. Birse, Z. Phys. A **355**, 231 (1996).
[49] M. Harada and K. Yamawaki, Phys. Rep. **381**, 1 (2003).
[50] K. Kampf, J. Novotny, and J. Trnka, Eur. Phys. J. C **50**, 385 (2007).
[51] D. Djukanovic, J. Gegelia, and S. Scherer, Int. J. Mod. Phys. A **25**, 3603 (2010).
[52] S. Weinberg, *The Quantum Theory of Fields. Vol. 1: Foundations* (Cambridge University Press, Cambridge, England, 1995).
[53] L. H. Ryder, *Quantum Field Theory* (Cambridge University Press, Cambridge, England, 1985).
[54] E. Kyriakopoulos, Phys. Rev. **183**, 1318 (1969).
[55] E. Kyriakopoulos, Phys. Rev. D **6**, 2202 (1972).
[56] S. L. Glashow, Phys. Rev. Lett. **11**, 48 (1963).
[57] P. J. O'Donnell, Rev. Mod. Phys. **53**, 673 (1981).
[58] V. V. Anisovich, A. A. Anselm, Y. I. Azimov, G. S. Danilov, and I. T. Dyatlov, Phys. Lett. **16**, 194 (1965).
[59] C. Becchi and G. Morpurgo, Phys. Rev. **140**, B687 (1965).
[60] J. W. Durso, Phys. Lett. B **184**, 348 (1987).
[61] I. Danilkin, O. Deineka, and M. Vanderhaeghen, Phys. Rev. D **96**, 114018 (2017).
[62] H. Gomm, O. Kaymakcalan, and J. Schechter, Phys. Rev. D **30**, 2345 (1984).
[63] O. Hajuj, Z. Phys. C **60**, 357 (1993).
[64] F. Klingl, N. Kaiser, and W. Weise, Z. Phys. A **356**, 193 (1996).
[65] M. Benayoun, L. DelBuono, S. Eidelman, V. N. Ivanchenko, and H. B. O'Connell, Phys. Rev. D **59**, 114027 (1999).
[66] P. D. Ruiz-Femenía, A. Pich, and J. Portolés, J. High Energy Phys. 07 (2003) 003.
[67] C. Terschlüsen, S. Leupold, and M. F. M. Lutz, Eur. Phys. J. A **48**, 190 (2012).
[68] Y.-H. Chen, Z.-H. Guo, and H.-Q. Zheng, Phys. Rev. D **90**, 034013 (2014).
[69] D. Kimura, T. Morozumi, and H. Umeeda, Prog. Theor. Exp. Phys. **2018**, 123B02 (2018).
[70] S.-L. Zhu, W.-Y. P. Hwang, and Z.-S. Yang, Phys. Lett. B **420**, 8 (1998).
[71] A. Gokalp and O. Yilmaz, Eur. Phys. J. C **24**, 117 (2002).
[72] C. Aydin, M. Bayar, and A. H. Yilmaz, Phys. Rev. D **81**, 094032 (2010).
[73] R. M. Woloshyn, Z. Phys. C **33**, 121 (1986).
[74] M. Crisafulli and V. Lubicz, Phys. Lett. B **278**, 323 (1992).
[75] C. J. Shultz, J. J. Dudek, and R. G. Edwards, Phys. Rev. D **91**, 114501 (2015).
[76] B. J. Owen, W. Kamleh, D. B. Leinweber, M. S. Mahbub, and B. J. Menadue, Phys. Rev. D **92**, 034513 (2015).
[77] C. Alexandrou , L. Leskovec, S. Meinel, J. Negele, S. Paul, M. Petschlies, A. Pochinsky, G. Rendon, and S. Syritsyn, Phys. Rev. D **98**, 074502 (2018).
[78] A. Cherman, T. D. Cohen, and R. F. Lebed, Phys. Rev. D **86**, 016002 (2012).
[79] T. D. Cohen, Rev. Mod. Phys. **68**, 599 (1996).
[80] R. K. Bhaduri, *Models of the Nucleon: From Quarks to Soliton* (Addison-Wesley, Redwood City, CA, 1988), Sec. 5.6.
[81] A. V. Manohar, in *Probing the Standard Model of Particle Interactions. Proceedings of the Les Houches Summer School, Session 68*, edited by R. Gupta, A. Morel, E. de Rafael, and F. David (Elsevier, Amsterdam, 1999), Pt. 1 and 2.
[82] H. W. Fearing and S. Scherer, Phys. Rev. D **53**, 315 (1996).
[83] O. Bär and U. J. Wiese, Nucl. Phys. **B609**, 225 (2001).
[84] P. A. Zyla *et al.* (Particle Data Group), Prog. Theor. Exp. Phys. **2020**, 083C01 (2020) and 2021 update.
[85] J. D. Bjorken and S. D. Drell, *Relativistic Quantum Mechanics* (McGraw-Hill, New York, 1964).
[86] C. Itzykson and J. B. Zuber, *Quantum Field Theory* (McGraw-Hill, New York, 1980).
[87] Wolfram Research, Inc., Mathematica, Version 11.0, Champaign, IL (2016).
[88] S. Okubo, Phys. Lett. **5**, 165 (1963).
[89] G. Zweig, CERN Report No. TTH-401 and No. TH-412, 1964 (unpublished).
[90] J. Iizuka, Prog. Theor. Phys. Suppl. **37**, 21 (1966).
[91] A. Manohar and H. Georgi, Nucl. Phys. **B234**, 189 (1984).
[92] E. E. Jenkins, A. V. Manohar, and M. B. Wise, Phys. Rev. Lett. **75**, 2272 (1995).
[93] J. Bijnens, P. Gosdzinsky, and P. Talavera, Phys. Lett. B **429**, 111 (1998).
[94] D. Djukanovic, J. Gegelia, A. Keller, S. Scherer, and L. Tiator, Phys. Lett. B **742**, 55 (2015).
[95] A. Krasniqi, H. C. Lange, and S. Scherer (to be published).